TECHNISCHE UNIVERSITÄT WIEN

MEDIZINISCHE UNIVERSITÄT WIEN

DIPLOMARBEIT

# Influence of Dose-Volume and Clinical Parameters on Patient-Reported Skin Toxicities in Breast Cancer Radiotherapy

zur Erlangung des akademischen Grades

**Diplom-Ingenieurin**

im Rahmen des Studiums

**Technische Physik**

eingereicht von

**Alice Arnold**
Matrikelnummer: 11901966

ausgeführt am Atominstitut
der Fakultät für Physik der Technischen Universität Wien
(in Zusammenarbeit mit der Medizinischen Universität Wien)

Betreuung
Betreuer: Priv.-Doz. Mag. Peter Kueß, PhD
Mitwirkung: Priv.-Doz. Mag. Barbara Knäusl, PhD Priv.-Doz. Gerd Heilemann, MSc PhD

Wien, 23.10.2025

(Unterschrift Verfasserin) (Unterschrift Betreuer)

## Abstract

Radiation-induced skin toxicities are one of the most common side effects that occur during radiotherapy for the treatment of breast cancer. This study investigated the influence of dose-volume metrics and clinical parameters on Patient Reported Outcome (PRO) of the following toxicities: skin dryness, itching, radiation skin reaction, skin darkening, and breast swelling and tenderness. The PROs were collected on a 5-point scale for acute and long-term side effects up to 24 months after treatment.

The analysis aimed to compare the severity of PROs and the change from the individual baseline of a patient for skin toxicities. The cohort included 1,138 patients, who were treated with radiotherapy during 2020–2024 at the Department of Radiation Oncology at the Medical University of Vienna / General Hospital of Vienna. The treatment techniques included the following three photon based external beam radiation techniques: Three-Dimensional Conformal Radiation Therapy (3D-CRT), Intensity-Modulated Radiation Therapy (IMRT), and Volumetric Modulated Arc Therapy (VMAT). These techniques differ in beam number, orientation and modulation, which may influence skin dose and PROs. An additional dose (boost) given to the surgical site, where the tumor was removed, was also considered as there was a recent transition from a sequential boost (SQB) to a simultaneous integrated boost (SIB). The treatment integration of those two boost methods differ, as the SIB is included during the main treatment, whereas the SQB is administered afterwards.

In *Experiment 1*, the severity of PROs was analyzed using a Kruskal-Wallis test, followed by a Dunn's Post-hoc test. The analysis compared groups defined by the treatment technique (3D-CRT, IMRT, or VMAT) and boost method (no-boost, SIB or SQB). In *Experiment 2*, logistic regression was used to examine the influence of dose-volume metrics and clinical factors (age, systemic therapies, prior surgery and treatment laterality) on the worsening of acute side effects from baseline before treatment. An event of worsening was defined as an increase from baseline of two or more points. In *Experiment 3* the long-term side effects from 6, 9, 12, and 24 months after the completion of the radiotherapy were investigated with the same predictors and event definition as before using a Cox proportional hazards model.

*Experiment 1* revealed that the most common reported score for acute skin toxicities was 2 (mild) across all groups. Severe (4) and very severe (5) PRO were mostly below 15% and 5% respectively. Overall more severe patient-reported skin toxicities were observed in groups treated with a SQB. Further logistic regression analysis in *Experiment 2* revealed that a larger high-dose skin volume was associated with more worsening events in acute side effects, while higher age reduced this risk. For long-term effects, which were investigated in *Experiment 3* no significant predictor could be found across all toxicity

items.

Assessing and aiming to minimize high-dose skin volumes during treatment planning could be beneficial in reducing acute radiation-induced toxicity. The relationship between high-dose skin volumes and skin toxicity was less pronounced than expected, as no correlation with late toxicities was observed for $V_{40\mathrm{Gy}}$.

## Zusammenfassung

Strahlungsinduzierte Hautnebenwirkung zählen zu den häufigsten Nebenwirkungen, die bei der Behandlung von Brustkrebs mit Strahlentherapie auftreten. Die Hautdosis sowie weitere klinische Faktoren können diese Nebenwirkungen beeinflussen. In dieser Studie wurde der Einfluss von Dosis-Volumen Metriken sowie klinischen Parametern auf die Nebenwirkungen, welche von Patientinnen und Patienten auf einer 5-stufigen Punkteskala berichtet wurden, untersucht. Dabei wurden folgende fünf Nebenwirkungen miteinbezogen: Trockenheit der Haut, Juckreiz, Hautverbrennung nach einer Bestrahlung, ungewöhnliche Verdunkelung der Haut und Schwellung oder Druckempfindlichkeit der Brust.

Die Analyse zielte darauf ab, den Schweregrad der berichteten Nebenwirkungen und die Veränderung gegenüber dem individuellen Ausgangswert für akute und langfristige Toxizitäten zu vergleichen. Die Kohorte umfasste 1,138 Patientinnen und Patienten, welche zwischen 2020 und 2024 an der Universitätsklinik für Radioonkologie der Medizinischen Universität Wien / Allgemeines Krankhenhaus Wien strahlentherapeutisch behandelt wurden. Die Behandlungstechniken umfassten dabei folgende drei photonenbasierte Teletherapien: Dreidimensionale Konformale Strahlentherapie (3D-CRT), Intensitätsmodulierte Strahlentherapie (IMRT) und Volumen- Intensitätsmodulierte Bestrahlung (VMAT). Diese Techniken unterscheiden sich durch die Anzahl, Form und Ausrichtung der Bestrahlungsfelder, wodurch die Hautdosis unterschiedlich ausfällt. Eine zusätzliche Strahlendosis auf das Tumorbett (Boost) kann als Teil der Bestrahlung erfolgen. Die Technik dieses Boosts wurde während der Beobachtungsperiode von einem Sequenziellen Boost (SQB) zu einem Simultan Integriertem Boost (SIB) umgestellt. Ein SIB wird integriert während der Hauptbestrahlung durchgeführt, wogegen ein SQB erst nach der Hauptbestrahlung erfolgt und die Beehandlungsdauer um eine Woche verlängert. Der Effekt der unterschiedlichen Bestrahlungs- und Boostmethoden wurde in dieser Arbeit untersucht.

Im *1. Experiment* wurde der Schweregrad der akuten Nebenwirkungen in den Kombinationen aus Technik- und Boostgruppen mittels eines Kruskal-Wallis-Tests untersucht, gefolgt von einem Dunn Post-hoc Test. Im *2. Experiment* wurde die Verschlechterung der akuten Nebenwirkungen mit den individuellen Ausgangswerten der Patienten verglichen. Hierbei wurde für die Verschlechterung ein Event eingeführt, welches einer Verschlechterung um zwei oder mehr Punkte entsprach. Mittels logistischer Regressionsanalyse wurden signifikante Faktoren identifiziert. Folgende klinische Faktoren wurden dabei als Prädiktoren einbezogen: das Alter zu Therapiebeginn, systemische Therapien (Chemotherapie und Hormontherapie), vorangegangene Operationen sowie die Behandlungsseite. In *Experiment 3* wurden die langfristigen Nebenwirkungen 6, 9, 12 und 24 Monate nach Abschluss der Strahlentherapie mit denselben Prädiktoren und gleicher

Eventdefinition wie in *Experiment 2* unter Verwendung eines Cox-Proportional-Hazards-Modells untersucht.

Der am häufigsten berichtete Wert für akute Hauttoxizitäten war 2 (wenig), während hingegen starke (4) und sehr starke (5) Nebenwirkungen meist unter 15% bzw. 5% lagen. Insgesamt wurden schwerwiegendere Nebenwirkungen in Gruppen mit SQB beobachtet. Die logistische Regressionsanalyse ergab, dass ein größeres mit Hoch-Dosis bestrahltes Hautvolumen mit mehr akuten Events verbunden war, während das Risiko für Events mit zunehmendem Alter abnahm. In den Langzeitnebenwirkungen konnten in den meisten Fällen keine signifikanten Prädiktoren für die Nebenwirkungen festgestellt werden.

Durch das Einbeziehen der Hoch-Dosis Hautvolumina in der Behandlungsplanung könnte das Risiko für akute Nebenwirkungen gesenkt werden. Der Zusammenhang zwischen dem Hoch-Dosis Volumen und Hauptnebenwirkungen war weniger ausgeprägt als erwartet, da für $V_{40\mathrm{Gy}}$ keine Korrelation mit den Nebenwirkungen beobachtet wurde.

## Acknowledgments

I want to thank my supervisors Barbara Knäusl and Gerd Heilemann, for their support and time for the many lively discussions on Monday mornings. My sincere thanks also go to Peter Kueß for enabling this thesis within the exciting field of radiation oncology and the opportunity to carry out my work at the Department of Radiation Oncology of the Medical University Vienna.

For their help, when I encountered technical issues, especially those related to RayStation scripting, I would like to thank Lukas Zimmermann and Leo Andexlinger. Further I want to express my appreciation to the PhD students from CDL IRENE for their warm welcome whenever I worked in their office and during lunch breaks.

I consider myself lucky to have met so many amazing people during my studies, who made this time so wonderful, both in- and outside university. Finally, I would like to thank my friends and family for their continuous support and encouragement!

# Contents

# 1 Introduction

Breast cancer is the most common cancer in women, with a global estimate of 2.3 million diagnosed cases and 670 000 deaths in 2022 [1]. Although breast cancer can also occur in men, they represent only about 1% of all treated cases [2]. Breast cancer diagnosis rates are higher in countries with a higher Human Development Index (HDI) compared to countries with a lower one. In regions with a very high HDI 1 in 12 women will be diagnosed with breast cancer during their life compared to regions with a low HDI where it is 1 in 27 [1]. Among women, breast cancer has an incidence rate of 43.4 per 100 000 — more than twice that of the next most common cancers [3]. Therefore the treatment of breast cancer remains one of the major challenges in modern healthcare, requiring continuous investigation of clinical and technical aspects to improve patient outcomes.

Treatment is based on factors like the cancer subtype, spreading outside of the breast tissue and individual factors. It is usually a combination of of surgery, radiotherapy and medication, such as chemotherapy, hormone therapy or antibody therapy [1]. In the US, around 95% of patients undergo surgery [4]. Globally it is estimated that radiation therapy should be used in 87% of cases according to treatment guidelines [5]. Two surgical options are available for patients: a breast-conserving lumpectomy, in which only the cancerous tissue is removed, and a mastectomy, in which the entire breast is surgically removed. The selection of the appropriate option is determined by the characteristics of the tumor. Following the surgical procedure, the presence of microscopic cancer cells remains a possibility. In order to reduce the probability of recurrence, radiotherapy treatment is administered [1]. The typical timeline for breast cancer therapy, with a focus on radiotherapy, is shown in the figure 1.1. In some cases, adjuvant therapies extend beyond radiation therapy.

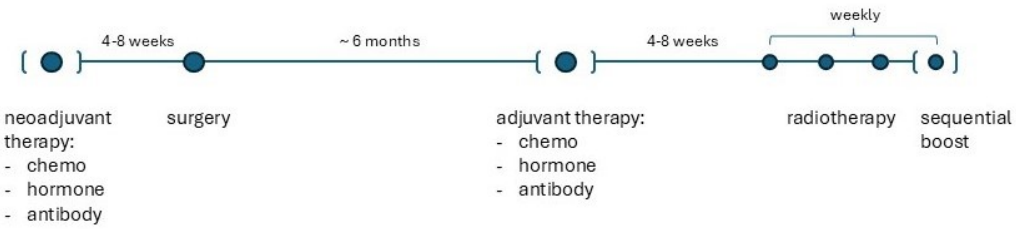


**Figure 1.1:** Timeline of breast cancer treatment at the Department of Radiation Oncology for patients who received radiotherapy. Systemic therapies and boost doses are administered when clinically indicated.

A defining characteristic of cancer cells is their higher rate of division and growth compared to normal cells in the body. In addition, the malignant cells possess the ability

to invade surrounding tissue and to spread to distant sites, a process known as metastasis. Radiation therapy is one of the most commonly used treatments to counteract this behavior. It involves depositing high-energy radiation from photons, electrons, or ions in the target tissue. This damages the DNA strands and leads to cell death. Although cancer cells are more susceptible to radiation damage than normal cells, minimizing radiation exposure to normal tissue is important because toxicities can occur [6]. One of the ways to minimize side effects from radiation on normal tissue is to split therapy into fractions over several weeks [7].

One of the main adverse effects associated with radiotherapy is the occurrence of acute radiation-induced skin reactions. The majority of patients, up to 95%, experience alterations in the skin. Severe reactions have been shown to impact the progression of the therapy and the quality of life [8]. Skin reactions can be grouped into acute adverse effects, which occur directly after the radiotherapy and late adverse effects which occur and last for weeks or months after completion of the treatment. The adverse skin reactions include reddening, itching, dry skin and changing of the skin structure [9].

In the past, clinician reported outcomes were primarily used to determine the side effects of radiation therapy. Recently, PROs have become increasingly used to determine side effects and their impact on the quality of life. With PROs it is possible to capture the patients experience and symptoms beyond clinical grading [10]. At the Medical University of Vienna the side effects are recorded using paper-based questionnaires completed in the clinic after the radiation therapy sessions, or electronically from home after completion of the treatment [11].

This study aimed to examine skin-related side effects following a radiation therapy. The studied side effects were reported by breast cancer patients from the Department of Radiation Oncology at Medical University of Vienna / General Hospital of Vienna. The influence of the absorbed skin dose on the side effects was studied. Further the impact of the following three treatment techniques: Three-Dimensional Conformal Radiation Therapy (3D-CRT), Intensity Modulated Radiation Therapy (IMRT), and Volumentric Modulated Arc Therapy (VMAT) (for definition see chapter 2.5) and the application of a higher dose to the tumor bed, called boost, was examined. These aspects are particularly interesting, since during the last four years two new radiotherapy treatment techniques were introduced and the boost method was changed from a sequential to a simultaneous integrated one in that time period. These changes were implemented to improve treatment quality as well as efficiency. The skin dose has not been systematically analyzed in this context at the Department of Radiation Oncology, as the skin is not automatically delineated as a structure in the Treatment Planning System (TPS).

One major task of this study was the transfer of patient data from the clinical database

to the research database for the generation of the skin structure in the Computed Tomography (CT) based 3D patient model and subsequent calculation of skin dose-volume metrics. Since data from more than 1,500 patients were included for transfer, an automated solution for exporting and importing the data between the databases had to be developed. As the data was used for research purposes, pseudonymization of patient information, such as the removal of personal identifiers, was implemented during the transfer process.

The differences in side effects between the baseline time-point at the day of the first fraction and immediately after radiation therapy were compared. Additionally, the relationship between skin dose and side effects was examined. It was assumed that the high-dose range is more relevant to side effects than the low-dose range. The influence of clinical confounders, such as concomitant therapies, age, and laterality, was investigated.

This thesis is structured as outlined below:

Section 2 introduces the physical, technological, and medical background in radiotherapy. It first explains the fundamentals of interactions of ionizing radiation with matter, which form the basic concepts of absorbed dose and dose distribution. Further, this section describes the principles of treatment planning and the different modalities used in breast cancer treatment. The statistical corrections employed for the experiments are described in the following subsections. Finally, an overview of the reported medical information about the patient cohort is provided.
Section 3 describes the treatment regimens applied. It also introduces the PRO from the Common Terminology Criteria for Adverse Events (CTCAE)-PRO catalog that was used to record the skin-related side effects. Further, the section outlines how patient data was transferred from the clinical to the research database, how skin structures were generated, and how dose-volume metrics were extracted. The three experiments are described: *Experiment 1* investigated the influence of treatment techniques and boost methods on the acute side effects. *Experiment 2* examined the correlations between acute patient-reported outcomes and dose-volume metrics. In *Experiment 3* the long-term side effects dependency on dose-volume metrics and clinical confounders was analyzed.
Section 4 presents the results of the study, beginning with data curation and descriptive analyses of the patient cohort, followed by the results of the three experiments.
In section 5, the results of the previous section are discussed and compared with findings in the literature.
Finally, Section 6 provides a summary and an outlook on future challenges.

# 2 Physical, Technological and Medical Background

## 2.1 Interaction of ionizing radiation

When high-energy particles pass through a medium, they interact with its atoms and transfer energy. The amount of energy deposited depends on the energy of the incoming particles and whether they carry charge. Neutral particles, such as neutrons and photons (X-rays and $\gamma$-rays), are classified as indirect ionizing radiation. Through their interaction with matter, they can produce directly ionizing particles. In contrast, charged particles such as protons, electrons, or heavier particles like $\alpha$-particles are classified as directly ionizing radiation, because they can ionize directly via collision, given their kinetic energy is high enough. The energy of the incoming charged particle is transferred in steps, resulting in an ionized track through the medium. Sometimes, this interaction leads to an ejected electron with enough energy to ionize, resulting in an ionization cascade [12].

In the following, this chapter will focus on the interactions of photons with matter, as this thesis evaluates treatment data of patients that were irradiated with photon radiation therapy. When a mono-energetic photon beam passes through a medium with a thickness of x, the beams intensity $I(x)$ is attenuated as in equation 2.1 where $I(0)$ is the initial intensity of the beam and $\mu$ the linear attenuation coefficient, which depends on the atomic number $Z$ of the medium and the photon energy $h\nu$ [13].

$$I(x) = I(0)e^{-\mu x} \tag{2.1}$$

There are five different ways which photons and matter can interact:

- Photo disintegration
- Coherent (Rayleigh) scattering
- Photo electric effect
- Compton effect (incoherent scattering)
- Pair production

Of the various types of scattering, only the photoelectric effect, pair production, and Compton effect are relevant for the energy ranges used in radiotherapy and will be discussed below. The energies used in radiotherapy lie below the threshold for photodisintegration to occur. In contrast, for coherent scattering to be a significant interaction path, the energy is required to be very low, which is not the case in radiotherapy [12]. The dominant regions for the cross sections of the three main effects are displayed in figure 2.2.

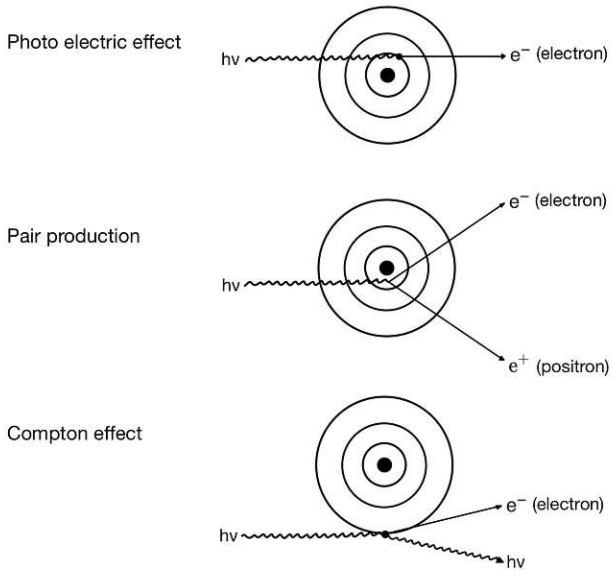


**Figure 2.1:** Schematic illustration of the three main interaction processes of photons with matter in radiotherapy. Illustration adapted from Choppin [15].

Photo electric effect: In the photoelectric effect, the photon has enough energy to eject a bound shell electron from an atom. The energy of the ejected electron $E$ is the difference between the energy of the photon $h\nu$ and the energy of the K-shell electron $E_k$: $E = h\nu - E_k$ [13].

Pair production: During pair production, the photon interacts with the Coulomb field of a nucleus, converting its energy into an electron-positron pair. The combined kinetic energy of the created pair is equal to $E_{KIN} = h\nu - 2m_e c^2$. For this process to occur, the photon must have a minimum energy of 1.02 MeV, which corresponds to twice the rest energy of an electron [13].

Compton effect: In the Compton effect a photon with a certain energy interacts with a quasi-free electron. During this interaction the energy of the photon $h\nu$ has to be larger than the binding energy of the electron. Part of the photon's energy is transferred to the electron, and it is scattered at angle $\theta$ [14].

During radiotherapy treatment the treatment machine's photons interact in a cascade of different ways before the dose is deposited inside the patient [17]. The main types of interactions are illustrated in the figure 2.3 below.

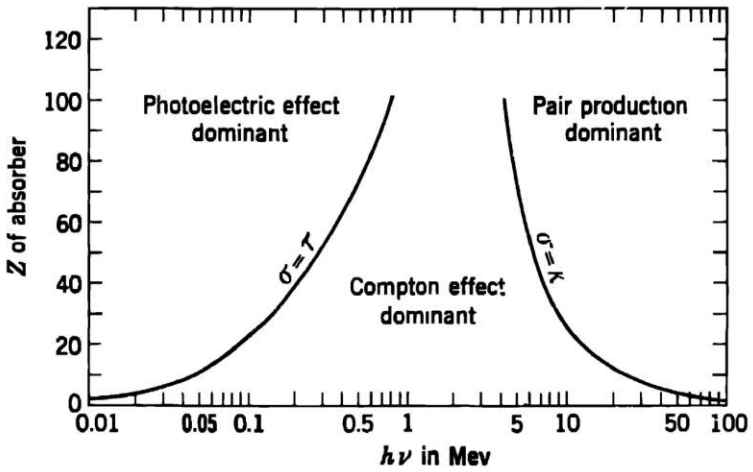


**Figure 2.2:** Dominant cross sections for the three main photon-matter interactions (photoelectric effect $\tau$, Compton effect $\sigma$, and pair production $\kappa$) as functions of the photon energy $h\nu$ and the atomic number $Z$ of the material. Figure taken from Evans [16].

## 2.2 Depth dose distribution of high-energy photons in water

For X-ray beams in water the maximum percentage depth dose is reached after the initial dose build-up, and afterwards the absorbed dose decreases, as shown in figure 2.4. The depth at which the maximum dose is reached depends on the energy and can range from a few millimeters for 4 MV to 5 cm for 25 MV. For low-energy beams, the maximum is very close to the surface. This dose build-up effect for higher energies can be used in therapy to spare the skin [18].

The dose buildup is explained by secondary electrons being ejected when a high-energy photon beam interacts with matter. These electrons travel a short distance before depositing most of their energy. As the photon beam penetrates deeper, the initial number of electrons set in motion increases, leading to a rising dose with depth. However, since the photon fluence gradually decreases due to attenuation, the production of new electrons decreases as well. The balance of these two effects creates a region of increasing dose, which reaches a maximum, after which the dose falls off [18].

The absorbed radiation dose is defined as the average energy deposited in a material of mass dm:

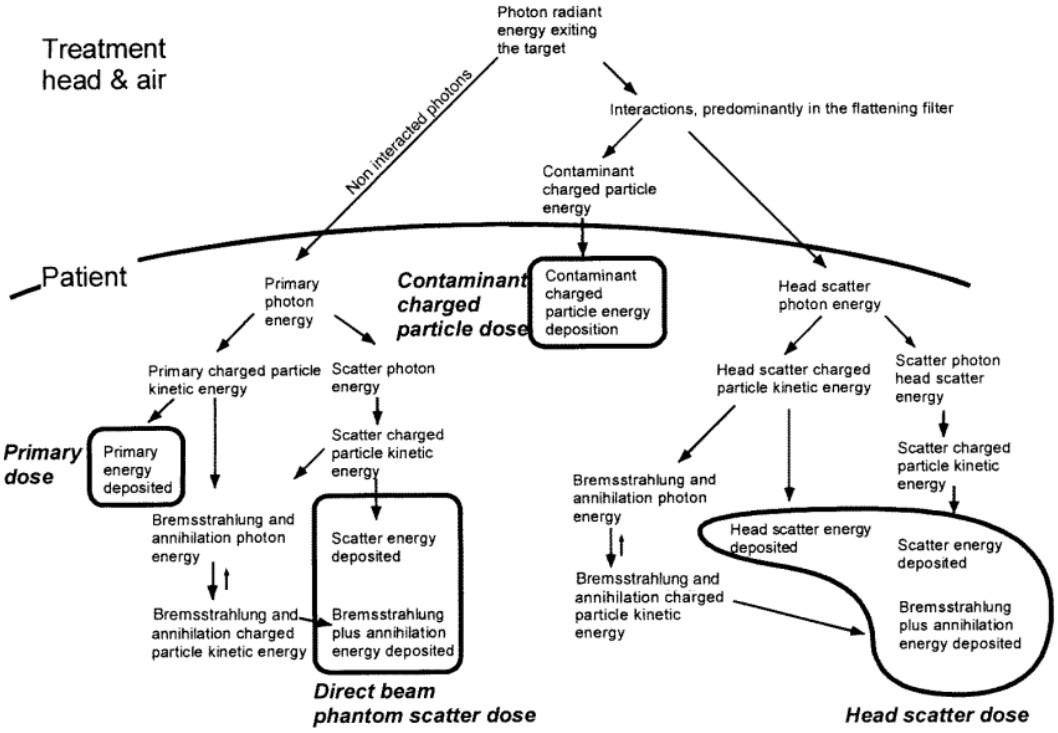


**Figure 2.3:** Interactions of a photon beam as it travels from the treatment head through the patient. Figure from Ahnesjö [17].

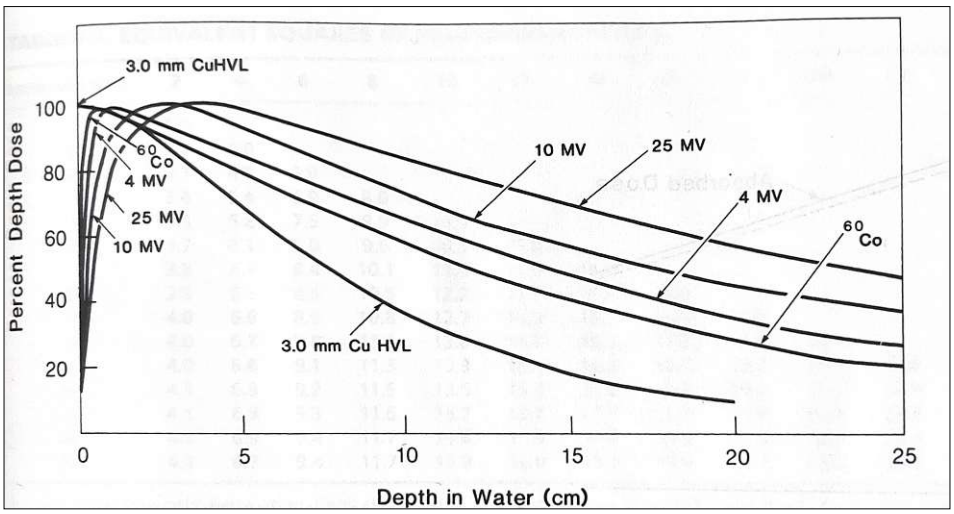


**Figure 2.4:** Depth dose distribution for the central beam axis for photon and $^{60}Co$ beams at different energies. Figure from Khan [12].

$$D = \frac{dE}{dm} \tag{2.2}$$

This quantity is expressed in units of Gray (Gy) [19]. However, it is almost never possible to measure the absorbed dose of a patient during radiation therapy. Therefore, dose distribution data is collected using water phantoms, as their absorption properties resemble those of soft tissue closely. This data is then used as the basis for dose calculation in the treatment planning process, which is described in chapter 2.4 [18].

## 2.3 Radiotherapy - concept and workflow components

Radiation therapy is one of the three pillars for cancer treatment and is applied in about half of all cancer cases [20]. The two main modalities of radiation therapy applied today to treat cancer are external beam radiation therapy and brachytherapy. During brachytherapy, radioactive material is placed inside the body via tubes for a short time period or seeds are implanted permanently [21]. External beam radiotherapy can be administered either by photons, electrons, protons or carbon-ions.

In external beam therapy using photons, with a typical energy of 4–18 MeV [22], the tumor is irradiated with high-energy photons accelerated with a Linear Accelerator (Linac) [13]. In the Linac a particle source at the end of a vacuum tube produces electrons, which are accelerated by electromagnetic waves in a straight trajectory. These electrons can be used for treatment or they collide with a target, producing X-ray photons that

are then used to irradiate the patient during treatment [13].

Protons are accelerated to energies between 70 and 250 MeV using cyclotrons or synchrotrons, and then used for treatment. Due to their characteristic energy deposition profile, protons offer clinical advantages over photons, particularly in sparing healthy tissue. However, proton therapy is less widely available and more costly. Consequently, the vast majority of cancer patients are treated with photons [22].

### 2.3.1 Target concepts

For radiotherapy treatment, usually three primary target volumes are delineated (see figure 2.5). These are defined independently of the treatment modality employed. The first is the Gross Tumor Volume (GTV), representing the visible and imageable extent of the tumor. The GTV is needed for Tumor-Node-Metastasis (TNM) staging, which is explained in chapter 2.6. The second is the Clinical Target Volume (CTV), which encompasses the GTV along with the surrounding region where microscopic disease spread may be present. The final volume is defined as the Planning Target Volume (PTV), which is understood as an expansion of the CTV to account for uncertainties in treatment planning and delivery. These uncertainties can arise from both internal and external factors. Internal uncertainties are caused by physiological motion, such as breathing, which can alter the shape, size and position of the CTV. External uncertainties, results from variations in the patient setup between treatment fractions and from mechanical instabilities of used equipment, such as sagging of the treatment couch [23].

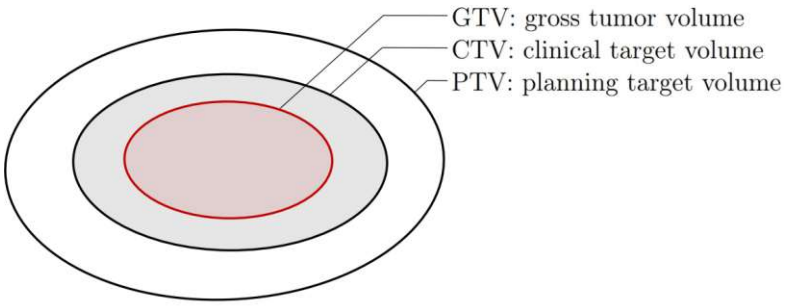


**Figure 2.5:** Illustration of the three main target volumes: GTV, CTV, PTV.

### 2.3.2 Pre-treatment workflow

The treatment workflow is a multistep procedure, which is depicted in figure 2.6. It begins with a physician's diagnosis and decision to treat with radiotherapy. Next, anatomical patient data is acquired through imaging with CT or other modalities [14].

The quantitative volumetric information of the patient is derived from CT imaging. These CT scans are used to generate a three-dimensional model of the patient, within which the PTV and the Organs At Risk (OAR) are delineated. The treatment plan is developed based on this 3D model, which includes calculations of beam attenuation [24].

Then, the planning processes for the treatment of radiotherapy begins by choosing the energy of the beams and the arrangement of the beams with the aim of delivering the prescribed dose to the target volume while sparing the surrounding OAR. For intensity-modulated treatment (see chapter 2.5.2), the weights of the beam segments are optimized to meet the constraints (dose limits) for OAR and to fulfill the dose prescription for the PTV. The treatment plan is evaluated, for example by analyzing the Dose-Volume Histograms (DVH). If the clinical goals or dose constraints are not met, the plan is adapted. Once the therapy plan fulfills all criteria, it is approved by the treating physician. The verification of the treatment plan can be performed either by an independent dose calculation or by measurements on the treatment machine [14].

The total prescribed dose, usually between 30 and 70 Gy, is delivered in fractions of 2 Gy, which corresponds to what is known as convectional fractionation. Splitting the total prescribed dose into fractions optimizes killing cancer cells while reducing toxicity to normal tissue. Typically, the irradiation of the fractions occurs over a period of 3–7 weeks, with five fractions per week [7].
A shorter treatment time with a higher single dose per fraction is referred to as hypofractionation. If the treatment is extended and the single doses per fraction are lower, this is referred to as hyperfractionation. For certain types of cancer, such as breast cancer, hypofractionation can be beneficial in some cases [7].

## 2.4 Dose calculation

In order to deliver the prescribed dose to the tumor, it is important to accurately calculate the deposited dose in the patient. This energy absorbed by the tissue is calculated using dose calculation algorithms. Ensuring that these calculation algorithms are both quick and accurate is crucial for guaranteeing timely and suitable treatment. There are three types of dose calculation algorithms: 1) factor-based, 2) model-based, and 3) principle-based (Monte Carlo (MC)) [25].

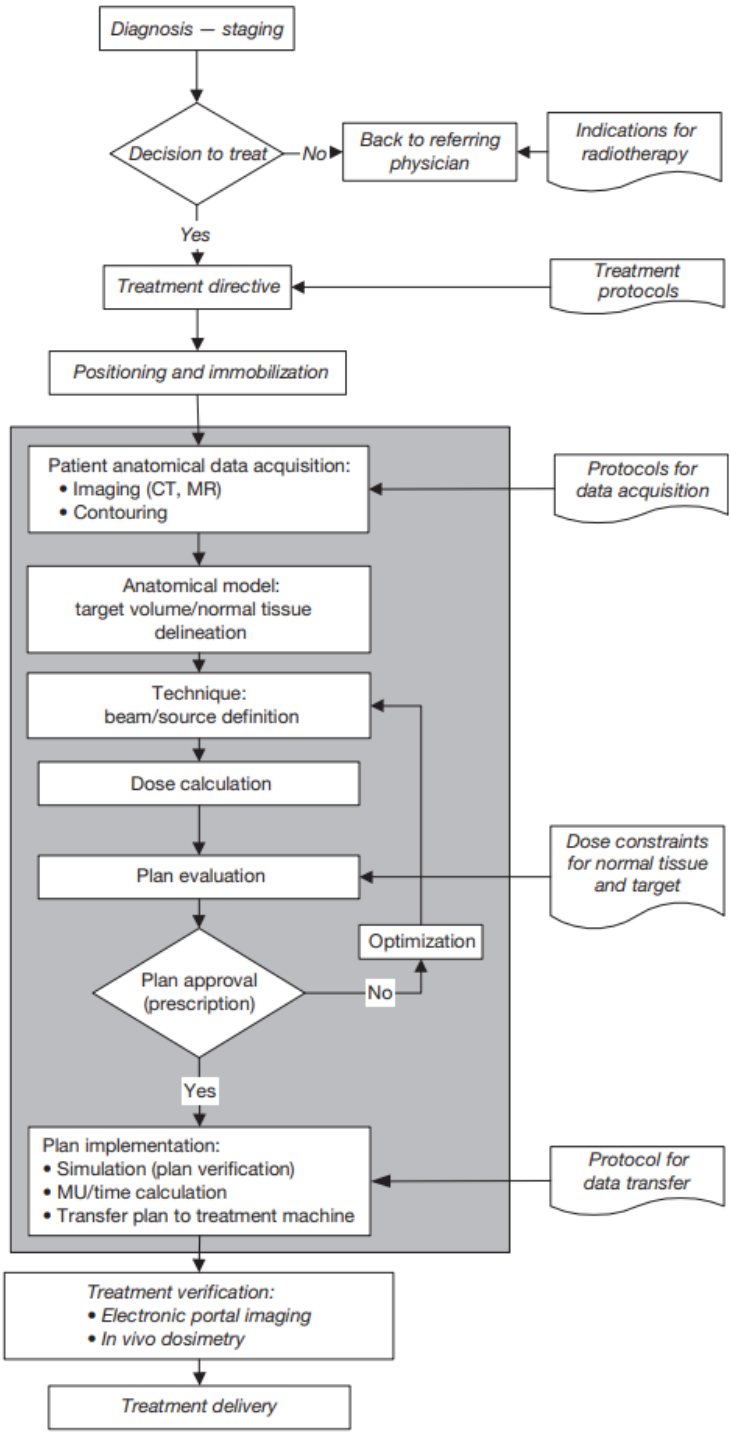


**Figure 2.6:** Treatment workflow. Figure from IAEA [14].

Factor-based dose calculation algorithms are among the earliest methods used for dose calculation in patients. These algorithms use measured data from water phantoms as basis. This data is then corrected using factors to account for the difference between water and patient tissue. The dose from the beam is measured at multiple settings (e.g., beam size, depth, and distance) within the phantom. To calculate the patient dose, correction factors are applied to these measured doses to account for different tissue densities in organs and curved surfaces. The simplest and fastest method to account for inhomogeneities is the 1D correction method, which only considers the beam's depth. However, this method does not take lateral scattering into consideration, so it is not very accurate. A slightly more advanced approach is the 3D correction method, which uses CT scans of patients. Factors-based algorithms are sometimes used to quickly check the calculated doses from other calculation methods. They are only used to get a rough estimate of whether the calculated doses are correct. The factor based method is not very accurate, especially for higher photon energies over 6 MV, since it does not model electron transport and scattering effects well [25].

Model-based algorithms are widely used by commercially available treatment planning systems, as they provide more accurate data than factor-based algorithms within a reasonable computation time. These algorithms use the energy fluence of the primary photons from the treatment machine. This energy is split into two components: Total Energy Released per unit MAss (TERMA) and the kernel. TERMA describes the energy released through interaction with tissue by primary photons from the Linac. The kernel represents how the energy spreads and is deposited around the interaction point of the primary photons by scattered photons and electrons. The total dose is calculated by summing the contributions from all interaction points. This is mathematically achieved through the convolution of TERMA $T(\vec{r}\,')$ and all dose kernels $k(|\vec{r}-\vec{r}\,'|, E')$:

$$D(\vec{r}) = \int dE' \int d^3\vec{r}\,' T(\vec{r}\,', E') k(|\vec{r}-\vec{r}\,'|, E') \tag{2.3}$$

TERMA $T(\vec{r}\,')$ depends on the linear photon absorption coefficient $\mu$, the mediums density $\rho$ and the energy fluence of the primary photons $\Psi$ as follows:

$$T(\vec{r}\,') = \frac{\mu}{\rho}(\vec{r}\,') \cdot \Psi(\vec{r}\,') \tag{2.4}$$

There are three main types of model-based algorithms. Pencil Beam Convolution (PBC) uses, as the name suggests, a pencil-shaped kernel, assuming that most of the scattering occurs along the beam direction. It is the fastest method, but not the most accurate for heterogeneous tissues. The second method is the Anisotropic Analytic Algorithm, an improved version of the PBC that includes lateral scattering. The kernel shape and

characteristics are derived from MC simulations. The third method is the Collapsed Cone Convolution. There the kernels are cone-shaped and radiate from the interaction point. This method is the most accurate of the three, but it is also the slowest. It is used by TPSs such as Oncentra MasterPlan (Nucletron, Inc., Columbia, MD, USA) and RayStation (RaySearch Laboratories AB, Stockholm, Sweden) [25].

Monte Carlo algorithms are the most detailed approach for dose calculation because they are based on the individual paths of photons and electrons passing through tissue. The MC algorithm is usually split into two steps: the beam simulation before entering the patient and the beam transport through the patient. The algorithm models the physical processes involved in transporting the beam through the patient. The accuracy of the calculation depends on precise information about the machine geometry and the number of particles used. A higher number of particles reduces statistical noise, but increases computation time. MC algorithms were long considered primarily as a benchmark for other calculation methods. However, recent improvements in computational power have made them increasingly feasible for routine clinical use [25].

## 2.5 Treatment concepts and techniques

The following section will describe the treatment concepts of Irradiation of the Whole Breast (WBI), Partial Breast Irradiation (PBI) and both boost methods, Simultaneous Integrated Boost (SIB) and Sequential Boost (SQB). Then three treatment techniques of external beam radiation therapy will be discussed in more detail: 3D-CRT, IMRT and VMAT.

In PBI the treatment dose is delivered to the tumor bed with an additional margin of 1–2 cm, whereas in WBI the full breast on side of the tumor is irradiated. With PBI the normal breast tissue is spared [26]. A boost dose is given to the tumor bed, where the malignant tissue has been surgically removed, in certain clinical situations. The purpose of this additional dose is to reduce the likelihood of an early recurrence, since most local recurrences tend to occur near the original tumor site [27]. SQB are delivered after the main treatment course is completed, whereas SIB are delivered simultaneously with the fractions of the main treatment. Therefore SQB extends the treatment duration.

### 2.5.1 Three-Dimensional Conformal Radiation Therapy

In the 1980s, the integration of CT imaging into radiation-based cancer therapy allowed to plan treatments based on three-dimensional data of both tumors and surrounding healthy structures [28]. This advancement led to the development of three-dimensional conformal radiotherapy (3D-CRT), in which radiation beams are shaped to match the target's outline and delivered with uniform intensity. However, 3D-CRT has limitations

in sparing critical structures in complex cases, especially when OAR are located near or within concave target volumes. The treatment is forward planned, which means that beam parameters are defined and can be adjusted manually. From these parameters, the dose distribution within the patient is then calculated [28].

### 2.5.2 Intensity-Modulated Radiation Therapy

In contrast, Intensity-Modulated Radiation Therapy (IMRT) varies the beam intensity across the field. Each beam is separated into beamlets with varying intensity levels. This allows for increased dose delivery to the tumor while minimizing exposure to nearby healthy tissue. In contrast to the forward planned 3D-CRT, IMRT uses inverse planning. Here, the dose distribution is specified first and the required beam intensities to achieve this distribution are determined by solving an integral equation. Unlike the generally convex dose distribution achieved with 3D-CRT, IMRT can also produce concave dose patterns that better conform to irregular tumor shapes. However, IMRTs low-dose regions are more spread out, due to a higher number of irradiation fields compared to 3D-CRT, which may lead to increased exposure of surrounding tissue [28].

### 2.5.3 Volumetric modulated arc therapy

In 2007, volumetric modulated arc therapy was first introduced. It is a type of IMRT in which the gantry is rotated around the patient, in contrast to the fixed angles used in IMRT and 3D-CRT. The dose is continuously delivered in 1-2 arcs [28]. Compared to the static beam techniques more skin volume is exposed to low radiation doses for VMAT.

## 2.6 Associated clinical parameters

To describe the breast cancer patient cohort, several clinical and pathological parameters were reported: age at therapy start, tumor grading, staging (including pathological T, N, and M categories as outlined below), morphology, receptor status, and Ki-67 expression. Treatment-related factors such as chemotherapy, antibody therapy, and hormone therapy will also be included. These factors can influence the occurrence and severity of side effects, they will be taken into account as potential confounders in the analysis.

The grade represents the tumor's potential for aggressiveness. Grades range from 1 to 3, with lower grades indicating less aggressive behavior than higher grades. The grade score is determined by factors such as the level of proliferation, differentiation, and shape of the tumor cells [29].

The TNM staging system is a worldwide system used to classify the anatomical extent of cancer [30]. Since the first published edition in 1977, it has been updated multiple times. The staging in this work is based on the 8th edition of the TNM staging system

[31], which was published in 2017.

There are two different staging methods: clinical and pathological. Pathological staging is based on removed tissue, whereas clinical staging uses tests or scans only [32].

The Tumor (T) stage describes the size and extent of the tumor. The scale ranges from T1 to T4, these groups can be divided into subgroups. Stages T1–T3 only describe the size. T1 describes a tumor with a maximum size of 2 cm, while T3 indicates a tumor bigger than 5 cm across. Stage T4 describes the spread of the tumor to nearby structures, such as the chest wall or skin. This includes Tis (DCIS), which describes pre-invasive breast cancer (ductal carcinoma in situ), in which cancer cells are confined to the breast ducts and have not spread to surrounding tissue [32].

The Node (N) stage indicates whether cancer cells have spread to the lymph nodes. The classifications range from pN0 to pN3. PN0 indicates that there are no cancer cells or only isolated cancer cell clusters with a diameter less than 0.2 mm in nearby nodes. From pN1 to pN3, the size of the cancerous tissue in the lymph nodes, as well as the number of affected lymph nodes, increases [32].

The Metastasis (M) stage indicates whether the cancer has spread to other parts of the body, such as the brain, lungs, liver, or bones. At the M0 stage, there is no indication that the cancer has spread beyond the original site. In the M1 stage, there are pathologically confirmed cancer clusters larger than 0.2 mm that have spread to different parts of the body [32].

Breast cancer is classified according to the presence of hormone receptors, including the Estrogen Receptor (ER), Progesterone Receptor (PGR), and Human Epidermal Growth Factor Receptor 2 (HER2). These receptors are proteins that bind the corresponding hormones and stimulate cell growth. Unlike the TNM staging, the status of these hormone receptors is either positive, meaning the cells express the receptors, or negative, meaning they do not. This classification is clinically important because such tumors can be effectively treated with the appropriate therapy [33].

Ki-67 is a protein found in the cell nucleus, and its score is used to determine cell proliferation and to predict response to chemotherapy. Ki-67 is assessed by staining the cells. The Ki-67 score measures the percentage of cells that are positively stained [34].

In most cases additional therapies, such as chemotherapy, hormone therapy or antibody therapy are administered alongside radiotherapy, which can influence the occurrence and severity of skin related side effects from radiotherapy. These therapies can be administered in two ways, neoadjuvantly, prior to surgery or adjuvantly, after surgery.

## 2.7 Statistical corrections for multiple testing

In statistical analysis the significance level $\alpha$ corresponds to the probability of falsely rejecting a true null hypothesis. With the conventional choice of $\alpha$=0.05, one would expect one false positive among 20 tested hypotheses. To account for the increased risk of error in multiple testing, the significance levels can be adjusted using the Bonferroni method. In the Bonferroni correction, the significance level, $\alpha$, is divided by the number of tests ($n$) performed. Alternatively, to obtain the adjusted p-values, the original p-value is multiplied by n [35].

A less conservative method than the Bonferroni method is the Benjamini-Hochberg procedure, where all p-values are ordered according to from smallest to largest. To obtain the corrected p-values the original p-values are multiplied with the total number of tests $n$ and dividing by their rank $r$:

$$p_{\text{corrected}} = p \cdot \frac{n}{r} \tag{2.5}$$

The largest p-value remains unchanged,the second largest turns into $p_{\text{correceted}} = p \cdot \frac{n}{n-1}$ [36]. A significant difference under the Bonferroni correction is also significant under Benjamini-Hochberg, since Bonferroni is always equal to or stricter than Benjamini-Hochberg.

# 3 Material and Methods

## 3.1 Study cohort curation

### 3.1.1 Inclusion and exclusion criteria

This study included patients from the Department of Radiation Oncology at the Medical University of Vienna / General hospital of Vienna who underwent radiotherapy treatment for breast cancer with curative intent from 2020 to 2024 and participated in the Patient Experience Data in Radiation Oncology (PEDRO) study (study number: EK 2184/2019) [11]. The following treatments were included in this thesis:

- Whole breast irradiation
- Partial breast irradiation
- Tumor bed boost: patients with and without boost irradiation
- Lymph node irradiation: patients with and without lymph node irradiation

Patients treated with palliative intent, where the aim is symptom relief rather than cure, and patients who underwent mastectomy and therefore, whose thoracic wall was irradiated during radiotherapy were excluded from this analysis.

### 3.1.2 Dose prescription, treatment scheme and techniques

At the Department of Radiation Oncology two treatment fractionation schemes are applied for breast cancer patients: ultra-hypofractionated irradiation applying 26 Gy in five fractions and moderate hypofractionated (40.05 Gy in 15 fractions). For this study, the patients receiving the ultrahypofractionated treatment scheme were excluded. All patients classified with an increased risk received an additional dose to the tumor bed. This boost dose was either prescribed simultaneously in 15×3.2 Gy (SIB) or subsequently in 4×2.5 Gy (SQB). A SIB did not change the number of fractions, whereas a SQB consisted of four additional fractions conducted after the 15 fractions of the main treatment were completed. The combinations of the different treatment schemes are displayed in the table 3.1 below. It includes the dose per fraction and the overall treatment dose.

Three different radiotherapy techniques, as described in chapter 2.5, were used for the selected patient collective: 3D-CRT, IMRT, and VMAT. In addition to radiotherapy, patients received various systemic therapies according to their individual needs. These included chemotherapy, hormone therapy, and antibody therapy.

Patients were categorized based on the treatment technique that accounted for the majority of delivered fractions. If the technique changed during treatment, only the

| Treatment scheme | Dose [Gy] and fraction | Total dose [Gy] |
|---|---|---|
| Ultrahypofractionated | $5.2 \times 5$ fx | 26 |
| Ultrahypofractionated + SQB | $5.2 \times 5$ fx + $2 \times 5$ fx | 36 (26+10) |
| Moderate hypo-fractionated | $2.67 \times 15$ fx | 40.05 |
| Moderate hypo-fractionated + SQB | $2.67 \times 15$ fx + $2.5 \times 4$ fx | 50.05 (40.05+10) |
| Moderate hypo-fractionated SIB | $3.2 \times 15$ fx | 48 |

**Table 3.1:** Treatment schemes including the fraction (fx) wise and total dose prescription.

dominant technique was considered; the boost method could differ from the main treatment technique but was not considered for categorization purposes. Information on the fraction number and technique were exported from MOSAIQ (Elekta AB, Stockholm, Sweden), the electronic record and verify system used at the Department of Radiation Oncology.

## 3.2 Patient-reported outcome measures

### 3.2.1 Survey schedule and item selection

Before the start of the radiotherapy each patient was asked wether they would like to participate in the PEDRO study. The base line fill-out of the survey happened on the day of the first radiotherapy treatment fraction, after the surgery and potentially systemic therapies, but before the first fraction was administered. The survey was filled out once a week during ongoing radiotherapy. After the completion of the radiotherapy treatment, PRO surveys were filled out in regular time intervals of 3, 6, 9, 12 and 24 months and subsequently once a year via a web application [11].

The survey questions followed the Patient-Reported Outcomes version of the Common Terminology Criteria for Adverse Events (PRO-CTCAE) catalog, which is a standardized tool used to evaluate symptomatic toxicities by self-report on therapy-related symptoms in cancer patients for clinical trials. The PRO-CTCAE catalog consists of 124 items which cover 78 different symptoms.

The items characterize frequency, severity, and presence or absence of toxicities including discomfort (pain, nausea, and fatigue) or skin reactions (swelling, blushing, and changes in skin structure). The answering scale depends on the question, it can be binary (1 yes, 2 no) or a scale ranging from 1–5 or 1–6 (1 not at all, 2 mild, 3 moderate, 4 severe, 5 very severe, 6 not relevant) [37]. This study focused on the following 5 items related to skin reactions: skin dryness, itching, radiation skin reaction, skin darkening, and breast swelling and tenderness. The survey questions of these 5 items are displayed in table 3.2.

| Item | Category | Question | Answer scale |
|---|---|---|---|
| 25_1 | Skin dryness | During the last 7 days: How DRY was your skin in the WORST CASE? | 1–5 |
| 28_1 | Itching | During the last 7 days: How STRONG was your ITCHING in the WORST CASE? | 1–5 |
| 36_2 | Radiation skin reaction | During the last 7 days: How pronounced were your SUNBURN-LIKE SKIN CHANGES AFTER EXPOSURE in the WORST CASE? | 1–6 |
| 37_1 | Skin darkening | During the last 7 days: Have you had an UNUSUAL DARKENING IN YOUR SKIN? | 1–2 |
| 72_1 | Breast swelling and tenderness | During the last 7 days: How STRONG was your BREAST SWELLING OR PRESSURE SENSITIVITY in the WORST CASE? | 1–5 |

**Table 3.2:** Skin-related items from the PRO-CTCAE.

### 3.2.2 Event definition

For each patient, the change in the PROs was calculated as the difference between the reported severity of each skin side effect item at baseline and at a later follow-up time after completion of the radiotherapy treatment. A positive value indicated an increase in severity, whereas a negative value indicated an improvement.

For each PRO item, a binary event variable was introduced. An event was defined as an increase of at least two points in the PRO item score between baseline and follow-up. In contrast to a difference of only 1, this definition suppresses noise more effectively. Item 37_1 (skin darkening) was an exception, because it was a binary item. A worsening of one score point was defined as an event because a worsening of two scores was not possible. With the introduction of events, the uncertainty about whether identical scores correspond to equivalent experiences or clinical outcomes across patients is reduced.

## 3.3 Data preprocessing and dose extraction

The patient data was available in the database of the clinical treatment planning system RayStation (Raysearch, Stockholm, Sweden). To generate the skin structure mask and export the corresponding dose data, the patient data had to be transferred to the research version of the Raystation TPS first. For this purpose, an automated pipeline was developed using scripts that run either inside RayStation or externally.

Recently treated patients were still available in the RayStation clinical database, while older ones were already stored in another database for long-term storage. In the first

step, patient data was exported from the clinical database to a hard drive in Digital Imaging and Communications in Medicine (DICOM) format, the standard format used internationally for medical imaging data [38]. A folder was created for each patient. All cases, examinations, treatment plans, and beam sets were looped through and the data was exported. Using the Pydicom [39] library on an eternal computer, patient-specific study instance UIDs and series instance UIDs were extracted for each patient. These unique identifiers (UIDs) were necessary for the automated import. This process had to be done outside the AKH workstations, as Pydicom was not available there.

The patient data was pseudonymized by replacing the patient name with a study code in the form of "PedroMamma00001", with increasing ending numbers. The pseudonymized patient data was then imported into the RayStation research database. To improve efficiency, both data export and import were performed in parallel using multiple RayStation instances simultaneously.

In the research database, an additional script, which was developed during my previous project work at the Department of Radiation Oncology, automatically generated the skin structure mask and updated the dose data. The skin thickness was set to 2 mm, as this is the average thickness in the body [40]. Dose-volume metrics were calculated by summing up the irradiated doses from each fraction within the patient structure. Information on the delivered fractions were obtained from the oncology information system MOSAIQ (Elekta AB, Stockholm, Sweden), as RayStation only stores the treatment plan and NOT the details on what was delivered. Changes or interruptions during the treatment are therefore not reflected in RayStation. Dose-volume metrics of the skin were derived by in-house developed scripts for the following dose-levels: 10 Gy, 20 Gy, 30 Gy and 40 Gy. The pipeline is illustrated in figure 3.1.

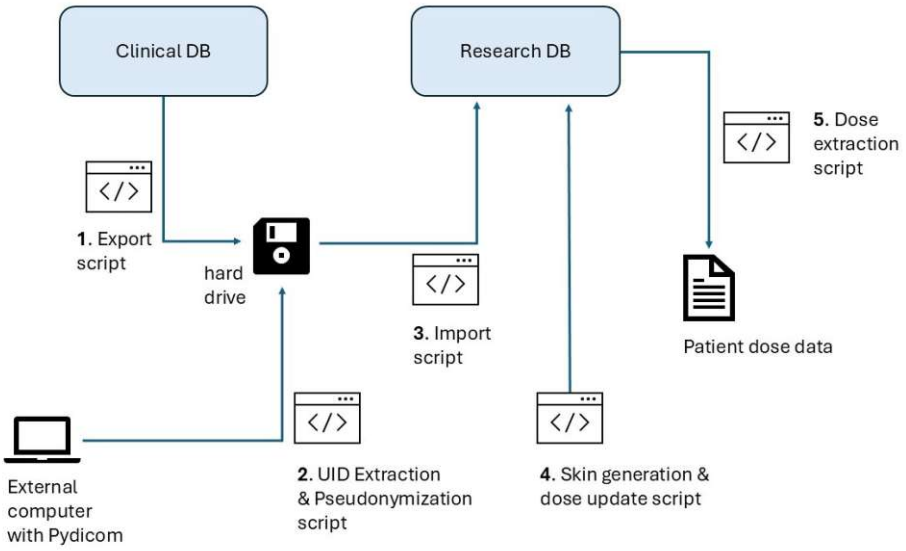


**Figure 3.1:** Patient export and import process including the export of the skin dose data.

## 3.4 Experiments

### 3.4.1 Experiment 1: Influence of irradiation technique and treatment scheme on the acute side effects

To study the severity of acute side effects, the PRO answers from the day of the last fraction were compared to the baseline values for groups combined by technique and wether patients received a boost or not. When the treatment included a boost irradiation, the boost method (SIB or SQB) was specified. The analysis only considered patients who completed all radiotherapy fractions. Incomplete irradiations would result in lower doses to the target and OAR than the prescription, which in turn could lead to under-reporting of the severity of the side effects. Following eight groups were analyzed:

- 3D-no boost [1]
- 3D-SQB
- IMRT-no boost
- IMRT-SIB
- IMRT-SQB
- VMAT-no boost
- VMAT-SIB
- VMAT-SQB

[1] When used in combination with a boost method, 3D-CRT is shortened to 3D.

PBI was excluded from the main analysis because it involves a smaller total irradiated volume and therefor also a smaller irradiated skin volume compared to WBI. Unlike WBI, the peripheral regions of the breast are not treated in PBI, which potentially leads to fewer skin side effects. In addition, PBI was not evenly distributed across all treatment techniques and boost methods. Including these cases in the main analysis would therefore introduce bias, as PBI represented an additional influencing factor. For this reason, PBI is discussed separately in chapter 4.2.2 of the results.

The differences for the acute skin related side effects were analyzed by performing a Kruskal-Wallis test using Phython's SciPy package [41] for each of the five question items. This method was chosen since the PRO answering scale is non-continuous and not distributed normally. When a significant difference was found between groups, the groups were compared pair by pair using a Post-hoc Dunn test to see which groups differ significantly from each other.

With seven groups (IMRT-SIB was excluded due to small group size; see chapter 4.2.1) and a pairwise comparison, $n$ equaled 21 in this experiment. This causes the Bonferroni significance level to decrease from 0.05 to 0.0024. The p-values were corrected with a second method: the Benjamini-Hochberg procedure [36]. This was implemented to detect more subtle effects, which could be disregarded by the Bonferroni method.

### 3.4.2 Experiment 2: Correlation between acute PRO and dose-volume parameter

This experiment aimed to investigate the relationship between irradiated skin volume and acute side effects. Instead of the severity the dichotomized worsening event variable was used. It also examined how other factors, such as age, systemic therapies, and prior surgery, influenced these side effects.

Multivariate logistic regression analysis was performed, as this model is suitable for assessing the binary outcome of worsening or non-worsening before and after the treatment for each of the 5 PRO items. The predictors included were: the skin volume which received 40 Gy ($V_{40\mathrm{Gy}}$) and the patients age as continuous variables, and laterality, surgery, chemotherapy, and hormone therapy as binary variables (coded as 1 = yes, 0 = no or 1 = right, 0 = left). These clinical predictors were selected in consultation with a physician. All statistical analyses were performed in Python using the "statsmodels" package [42].

Prior to the logistic regression analysis, a Spearman correlation test was performed to determine the correlation strength between skin volumes of different dose levels (10 Gy, 20 Gy, 30 Gy, and 40 Gy) and side effects. Since these dose parameters are correlated only one should be used for further analysis.

For this experiment, patients who reported side effects of a score of 4 (severe) or 5 (very severe) at baseline were excluded to avoid a bias not related to the radiotherapy treatment. Unlike in *Experiment 1*, unfinished therapies with less than the foreseen 15 or 19 fractions (without or with a boost) were included, as the lower dose that was received by the skin was directly included as dose-volume metrics in the analysis. Further, patients who were treated bilaterally were excluded for this analysis and *Experiment 3*.

$N$ was equal to 6 , as it corresponded to the number of predictors used in the logistic regression. Therefore the corrected significance level was 0.0083.

### 3.4.3 Experiment 3: Long-term side effects

The predictors for late side effect worsening were investigated using Cox proportional hazards models. The definition of an event was the same as in *Experiment 2*: the worsening of the PRO score of two or more from the baseline was defined as an event. For the long-term toxicities the included follow-up time points were: 6, 9, 12, and 24 months. The 3 month follow-up time was excluded, as acute side effects may still be present at that time and influence the PRO score. The definition of acute adverse effects is the occurrence of those up to three months after the radiotherapy, while toxicities occurring after that time period are classified as long-term toxicities. The distinction between the two is based on different physiological mechanisms [43].

Before conducting the statistical analysis, the number of completed questionnaires was reviewed to assess the amount of available data. The analysis also examined how many patients stopped participation or missed interim surveys. The exclusion criteria for this analysis were the same as in *Experiment 2*.

The probability of event free survival was visualized with Kaplan-Meier curves. Both the Cox proportional hazards modeling and the Kaplan-Meier curves were carried out in Python using the lifelines library [44]. $N$ was equal to 6 , as the same predictors were used as in *Experiment 2*. Therefore, the significance level was 0.0083.

# 4 Results

## 4.1 Data curation of the patient cohort

From August 2020 to October 2024, 1,523 breast cancer patients received radiotherapy treatment at the Department of Radiation Oncology. Of this patient cohort, 1,480 patients were successfully transferred from the database of the clinical TPS to the database of the research system. For 1,466 of the successfully transferred patients a skin structure could be generated. Ultimately, the dose could be exported for 1,380 patients. This group included all breast cancer patients independently of the treatment scheme, moderate and ultrahypofractionated patients.

The slowest step in this process was exporting data from the clinical or long-term storage database. The duration of the export of 50 patients was recorded twice. Depending on the amount of patient data, the execution time varied. The first export run of 50 patients took 95 minutes, which resulted in an average time of 1 minute and 54 seconds per patient. The second run took 130 minutes which corresponds to an average of 2 minutes and 36 seconds per patient. During the import to the research database, the batches of 50 patients took 35 minutes and 72 minutes.

## 4.2 Descriptive results

### 4.2.1 Patient cohort

The patient cohort for analysis included a total of 1,138 patients. As expected for breast cancer, the cohort consisted predominantly of females, with a very small proportion of males. Left- and right-sided cases were nearly equally distributed, with 566 cases on the left and 548 cases on the right side. In addition, 24 patients were treated on both sides. While the majority of patients underwent surgery prior to radiotherapy, a subgroup (less than 10%) received radiotherapy without surgery. Most patients received whole-breast irradiation (WBI), while approximately 10% received partial breast irradiation (PBI). However, patients who received PBI were not evenly represented among the technique subgroups. Only patients without the need for a boost irradiation received PBI with one exception. The PBI distribution shares ranges between 8% and 32% for the subgroups. In the 3D-CRT group, PBI treatment accounted for 32%, in the VMAT group for 20%, and in IMRT group for just 6%. This reflects the fact that, once the treatment technique shifted from 3D-CRT, VMAT offered greater advantages for PBI than IMRT did. The combination of IMRT and PBI was only used for a short intermediate period. The distribution of PBI is shown in table 4.3.

Approximately 40% of patients received chemotherapy. Two types of chemotherapy

| Technique | PBI count | Total patient count | Percentage |
|---|---|---|---|
| 3D-no boost | 62 | 195 | 32% |
| IMRT-no boost | 10 | 129 | 8% |
| VMAT-no boost | 31 | 142 | 22% |
| VMAT-SIB | 1 | 138 | <1% |

**Table 4.3:** Distribution of PBI. Groups that are not listed were treated with WBI only.

were administered: neoadjuvant and adjuvant. More than 65% of patients received hormone therapy, while fewer than 5% received antibody therapy. Figure 4.1 summarizes the information on the patient cohort.

The composition of the patient cohort by radiation technique and boost method is summarized in the following table 4.4. The three treatment technique groups were similar in size, with 447 3D-CRT patients, 329 IMRT patients, and 362 VMAT patients. In contrast, the distribution of the different boost methods was uneven. The SIB group, with 176 patients, was significantly smaller than the other two groups: 487 patients in the SQB group and 475 patients in the no-boost group.
The resulting subgroups (defined by the combination of treatment technique and boost) ranged from 36 to 246 patients. As expected, there were no patients in the 3D-SIB subgroup, since SIB was technically not feasible with 3D-CRT and was only introduced after the 3D-CRT technique became outdated. The smallest non-empty subgroup was IMRT-SIB, with 36 patients, which reflects the short time this combination was in use. Due to the small size, this group was excluded from *Experiment 1.*

| | 3D-CRT | IMRT | VMAT | Total |
|---|---|---|---|---|
| SIB | 0 | 36 | 140 | 176 |
| SQB | 246 | 163 | 78 | 487 |
| No-boost | 201 | 130 | 144 | 475 |
| Total | 447 | 329 | 362 | 1138 |

**Table 4.4:** Matrix of the patient cohort with treatment technique and boost method.

During the inclusion period for this study (August 2020 to October 2024), the treatment techniques and the boost method changed. Initially, all patients were treated with 3D-CRT. VMAT was introduced in August 2021, followed by IMRT around six months later, which gradually replaced 3D-CRT. Between June and August 2023, VMAT increasingly replaced IMRT, and by September 2024, VMAT was the only treatment technique used. These changes are depicted in figure 4.2.

The boost method also changed from SQB to SIB during this time period. SIB was first introduced in September 2023 and completely replaced the SQB by February 2024. The shift to SIB was mainly due to its efficiency, as it enables the boost dose to be delivered during the main treatment, thereby reducing the overall therapy duration. The amount of patients who did not receive a boost stayed almost constant. The figure 4.3 shows the changes in the boost method over the observed four years.

| | |
|---|---|
| **Age** | |
| Median (IQR) | 57 (49-66) |
| Range | 24-92 |
| **Sex** | |
| Female | 1134 |
| Male | 4 |
| **Grading** | |
| G1 | 191 |
| G2 | 556 |
| G3 | 365 |
| Unknown | 26 |
| **Side of primary tumor** | |
| Left | 566 |
| Right | 548 |
| Bilateral | 24 |
| **Specification** | |
| Whole breast irradiation | 1029 |
| Partial breast irradiation | 107 |
| Unknown | 2 |
| **Pathological size of tumor stage (T stage)** | |
| PT0 | 122 |
| PT1 | 676 |
| PT2 | 182 |
| PT3 | 27 |
| PT4 | 0 |
| PTis | 102 |
| Unknown | 29 |
| **Pathological node stage (N stage)** | |
| PN0 | 758 |
| PN1 | 199 |
| PN2 | 50 |
| PN3 | 12 |
| Unknown | 119 |
| **Pathological metastasis stage (M stage)** | |
| PM0 | 442 |
| PM1 | 6 |
| Unknown | 690 |
| **Morpholohy** | |
| IDC | 832 |
| DCIS | 159 |
| ILC | 95 |
| Sonderform | 44 |
| Unknown | 8 |
| **Technique** | |
| 3D | 447 |
| VMAT | 362 |
| IMRT | 329 |
| **Boost** | |
| SQB | 487 |
| SIB | 176 |
| no boost | 475 |
| **Receptor Status** | |
| ER + | 919 |
| ER - | 212 |
| ER Unknown | 7 |
| PGR + | 802 |
| PGR - | 329 |
| PGR Unknown | 7 |
| HER2 + | 87 |
| HER2 - | 883 |
| HER2 Unknown | 12 |
| **Ki67** | |
| 0–20 | 639 |
| 21–40 | 223 |
| 41–60 | 116 |
| 61–80 | 94 |
| 81–100 | 48 |
| Unknown | 18 |
| **Chemotherapy** | |
| Yes | 417 |
| No | 721 |
| Neoadjuvant | 309 |
| Adjuvant | 132 |
| **Hormontherapy** | |
| Yes | 758 |
| No | 380 |
| **Antibodytherapy** | |
| Yes | 51 |
| No | 1087 |

**Figure 4.1:** Demographic, clinical and treatment characteristics of the patient cohort with n=1,138.The patients listed under Unknown at stage N correspond to patients who did not undergo surgery prior to radiotherapy, as classification of the N-stage can only be made in the course of surgery.

**Figure 4.2:** Monthly distribution of the treatment techniques for breast cancer patients.






**Figure 4.3:** Monthly distribution of the boost method for breast cancer patients.

### 4.2.2 Whole versus partial breast irradiation

Figure 4.4 shows the volumes which were irradiated with 10 Gy for WBI + PBI compared to WBI alone. The plot on the left shows both irradiation concepts, whereas PBI are excluded from the right plot. A double distribution becomes apparent in the three no-boost groups when WBI and PBI are grouped together. This effect is most pronounced in the 3D-no boost group, where the inclusion of 62 additional PBI cases introduced a cluster of lower volume values. The lower part of the distribution are predominantly the PBI patients, while the higher volume values are mainly associated with WBI patients. The skin volume irradiated with 10 Gy averaged 72 ($\pm$30) cm$^3$ for WBI and only 42 ($\pm$23) cm$^3$ for PBI in the 3D-no boost group. Since PBI patients received a lower average skin dose, less side effects were expected, these patients were excluded from further analysis.

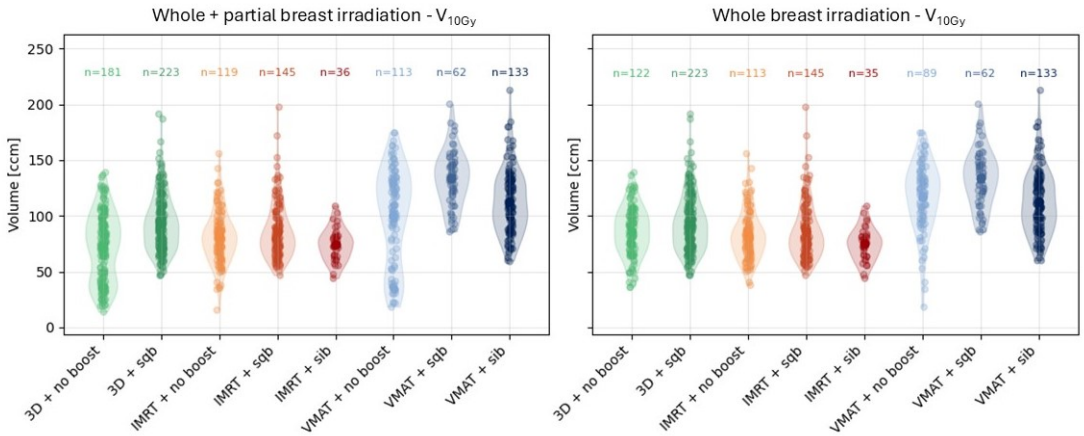


**Figure 4.4:** Comparison of volumes which received 10 Gy for partial and whole breast irradiation.

### 4.2.3 Boost versus No-Boost Comparison

The distribution of changes in the PRO skin side effects with and without a boost were compared. The analysis included 655 patients in the boost group and 363 patients in the group without a boost. The boost group included patients who received either SQB (482) or SIB (173) treatments. Note that the treatment course for SQB patients was approximately one week longer. Further only patients who completed the full treatment course were included in the cohort. Patients treated with PBI were excluded for this analysis.

For each of the 5 skin items a histogram plot with the changes between the baseline and after the completion of the radiotherapy treatment are displayed in figure 4.5. The height of the histograms represent the percentage of patients from the boost or no-boost group who reported worsening, improvement or no change from baseline. Across all items the majority of patients reported no or slight changes from baseline -1 to +1. Overall, a tendency towards worsening can be observed, rather than improvement, which is consistent with expectation. There was a difference between the two groups: patients in the boost group reported worsening more frequently than patients in the no-boost group. For the improvements the trend was reversed, as more patients treated without a boost reported improvements more often (negative values).

For the items 36_2 (radiation skin reaction) and 72_1 (swelling and tenderness) the distribution differed from the other items in that they were centered between 0 and +1 rather than around 0. In particular for item 36_2, the most common change was a worsening of +1 for both the boost and no-boost group, with 30% and 32% .
The biggest difference between the boost and no-boost group can be seen in the plot for item 37_1 (skin darkening). Here 42% of boost patients reported a worsening compared to 28% in the no-boost group. As this was a binary item, the response option were limited to yes or no.

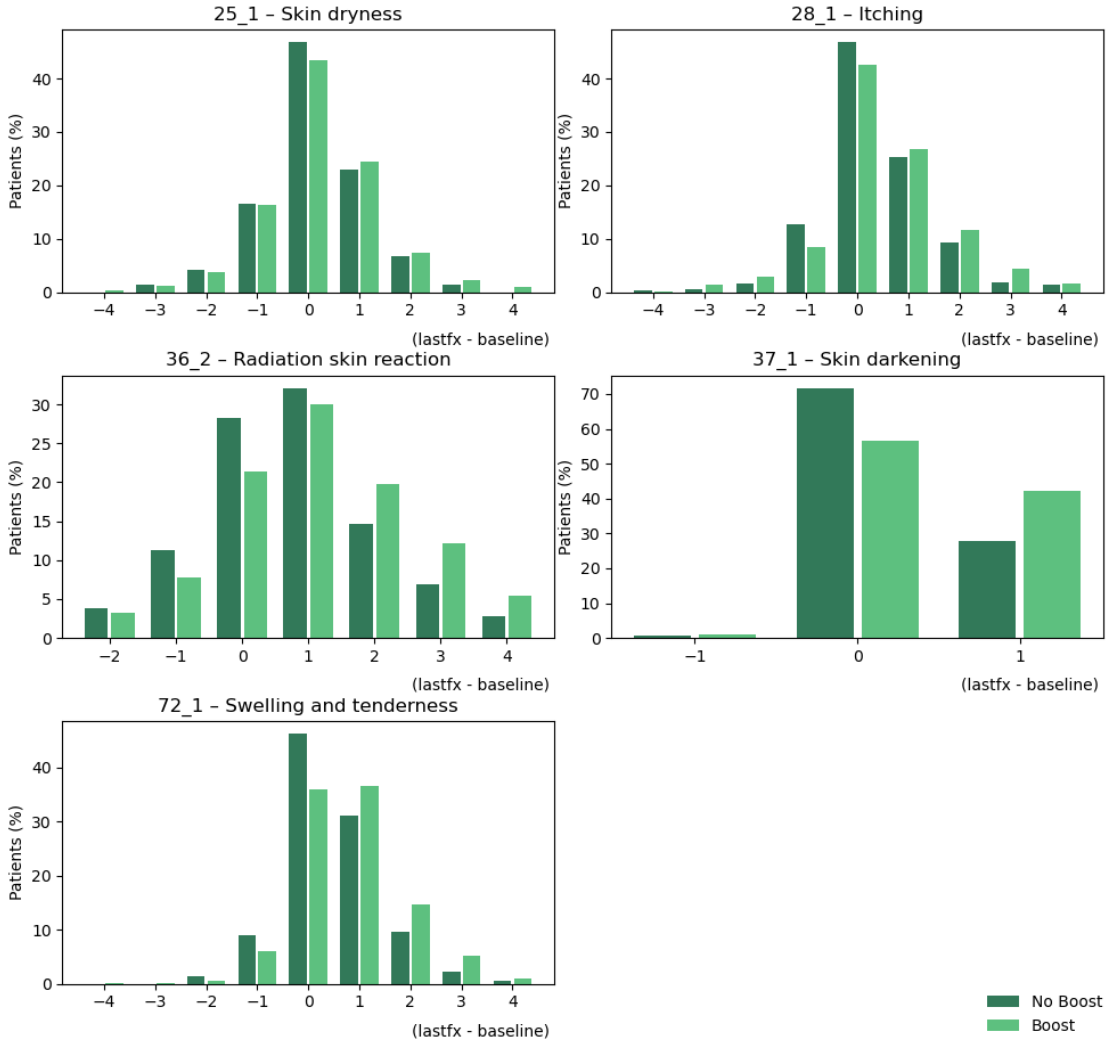


**Figure 4.5:** Change from baseline at the last fraction for the boost and no-boost treatment groups.

## 4.3 Experiment 1: Influence of irradiation technique and treatment scheme on the acute side effects

980 patients from the main cohort were included in the analysis of acute side effects for different treatment techniques and boost methods.

The table 4.5 lists the average PRO scores for all reported skin related side effect items. The most severe effects were observed for item 36_2 - radiation skin reaction, where the

mean of the reported scores after the last fraction ranged from 2.05–2.78. When comparing treatment technique-boost method groups, on average, the side effects were lowest in the no-boost groups across items. The VMAT-SIB group also reported similarly low side effects, whereas the groups with a SQB reported higher scores. When only VMAT plans were considered in the comparison between SIB and SQB, thereby eliminating the influence of different planning techniques, no significant difference was observed between the two boost methods, even though the boost volume received a higher fraction dose in the SIB.

At baseline, there were almost no significant differences between the groups, with an exception for item 25_1 (skin dryness), which is discussed in detail in section 4.3.1. In general baseline toxicities were lower compared to after the last fraction, with mean changes ranging from 0.03–1.31. The only exception is the 3D-no boost group for item 25_1, where a decrease from baseline to after the last fraction was observed.

The results of the individual items are described in the following sub-chapters which are structured as follows: The figures 4.6-4.10 show the frequencies of the reported scores per group at baseline and after the last fraction. The responses within each group were normalized to 100% for simpler comparison. Subsequent to the plots for each of the items is a table (4.6, 4.7, 4.8, 4.9, 4.10) containing the calculated raw p-values, the Benjamini-Hochberg corrected p-values, and the Bonferroni corrected p-values for all 21 pair-wise group comparisons.

| Technique | 25_1 | 28_1 | 36_2 | 37_1 | 72_1 |
|---|---|---|---|---|---|
| 3D-no boost | 2.11 (0.98) | 1.82 (1.04) | 2.15 (1.08) | 24.2% | 1.95 (0.95) |
| 3D-SQB | 2.29 (1.08) | 2.19 (1.15) | 2.68 (1.24) | 48.9% | 2.28 (1.08) |
| IMRT-no boost | 1.94 (0.92) | 1.90 (1.00) | 2.37 (1.07) | 35.3% | 2.06 (0.90) |
| IMRT-SQB | 2.31 (1.05) | 2.36 (1.21) | 2.78 (1.10) | 49.4% | 2.38 (1.13) |
| VMAT-no boost | 2.03 (0.99) | 1.69 (0.98) | 2.05 (0.95) | 23.6% | 1.95 (0.99) |
| VMAT-SIB | 2.04 (1.09) | 1.80 (0.92) | 2.36 (1.04) | 29.2% | 2.13 (0.95) |
| VMAT-SQB | 2.35 (1.18) | 2.05 (0.97) | 2.40 (1.12) | 44.2% | 2.09 (0.95) |

**Table 4.5:** Overview of all acute skin side effect after the last fraction. Reporting mean and standard deviation in brackets for the all items excluding 37_1. Item 37_1 had a binary answer score: whether or not patients experienced skin darkening. The reported percentage corresponds to the number of patients who answered "yes".

### 4.3.1 Skin dryness (25_1)

The baseline of the PRO for dryness of the skin is shown in the first plot of figure 4.6. For all groups between 35% and 49% of patients reported no skin dryness (score = 1) before radiotherapy treatment, indicating more than 50% of patients experienced mild (score = 2) to very severe skin dryness (score = 5). This pattern differed from all other assessed PRO-CTCAE items, where the majority of patients did not experience side effects at baseline.

Further, 5 pairwise group comparisons showed significant differences for skin dryness at baseline. In contrast, for all other items no statistical significant differences were observed with one exception. For item 28_1 one pairwise difference was observed, which is in more detail in chapter 4.3.2. For item 25_1, a significant difference under Bonferroni correction could be only observed between 3D-SQB and VMAT-SIB.
In the VMAT-SIB group, 47% of patients reported no dryness (score = 1), compared to only 35% in the 3D-SQB group. On the other hand, for higher severity levels (scores 2–5), a higher percentage of patients reported these levels in the 3D-SQB group than in the VMAT-SIB group.

The severity of skin dryness after the completion of the radiotherapy treatment is shown in the second plot of figure 4.6. Compared to the baseline the percentage that reported no skin dryness was reduced after radiotherapy across all groups. The IMRT-SQB group showed the greatest change, with the percentage of patients with score 1 severity falling from 40% to 23%. The increase to score 4 was especially large in the two VMAT boost groups, tripling from 5% to 15% for VMAT-SQB and increasing almost ten-fold from 0.7% to 6.6% for VMAT-SIB, corresponding to an increase from 1 to 9 patients.

The two groups with the highest percentage of patients, who reported no dryness were IMRT-no boost and VMAT-SIB, both with 36%. The main differences between those two groups were observed at scores 3 and 4. In the IMRT-no boost group, 19% of patients reported a score of 3 and 2% a score of 4, whereas in the VMAT-SIB group 11% reported a score of 3 and 7% a score of 4.

The highest levels of skin dryness were found in the VMAT-SIB and VMAT-SQB group, where around 5% reported the maximum severity (score = 5). In contrast, the lowest proportion of severe skin dryness was reported in the 3D-no boost group, with only 1.5%. No significant difference could be found between the VMAT-SQB and the VMAT-SIB group. This may be due to the smaller group size, as only responses of 77 patients were included in VMAT-SQB compared to at least 138 responses for all other groups. Overall, significant differences between groups were limited, with only four pairwise treatment group comparisons showing a statistically significant difference, which

is shown in table 4.6.

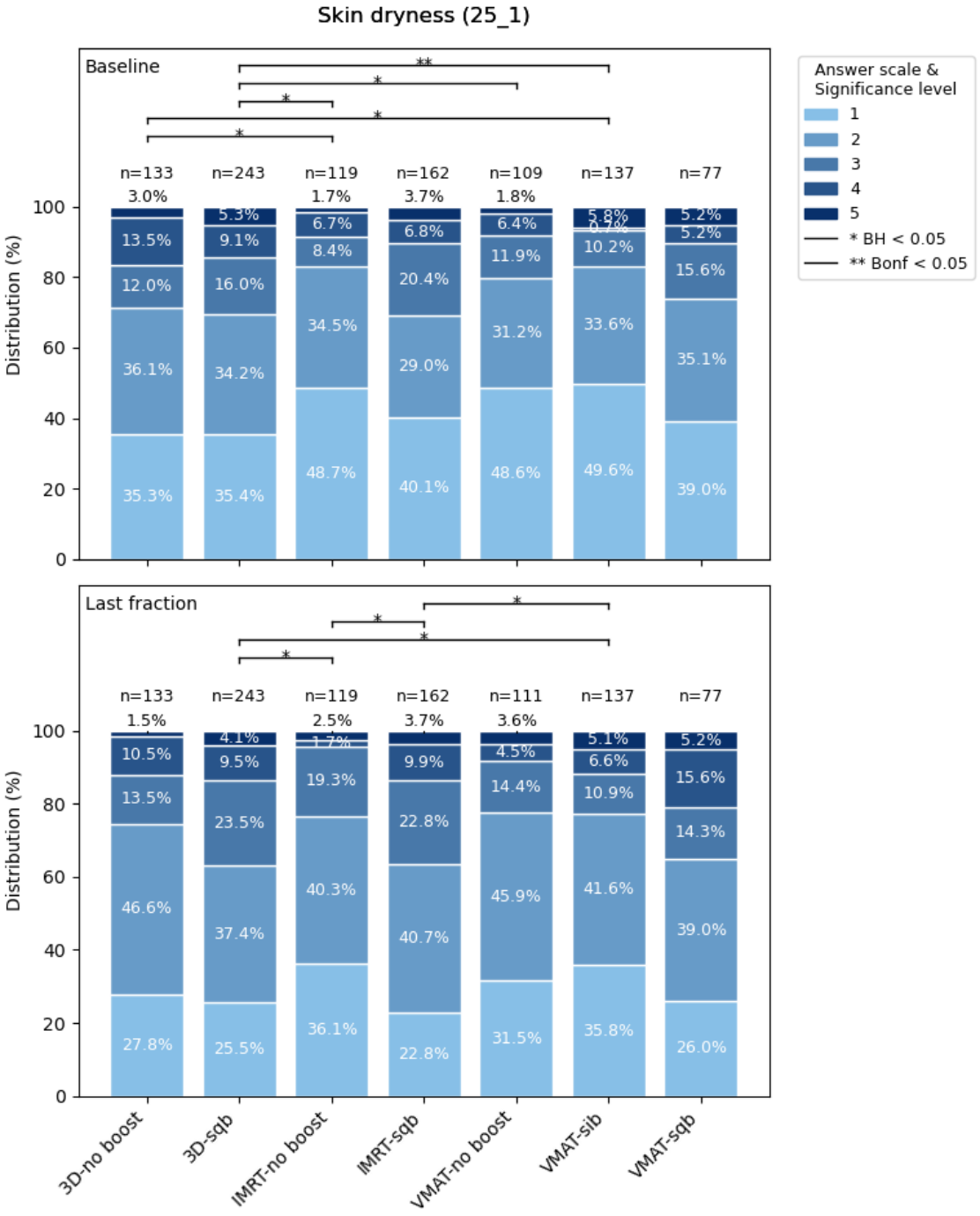


**Figure 4.6:** Normalized PRO frequencies for Item 25_1 at baseline and after treatment. Brackets above the histograms connect groups with significant differences after correction.

| Compared techniques | Raw p | BH p | Bonf p |
|---|---|---|---|
| 3D-no boost vs 3D-SQB | 0.1222 | 0.2333 | 1.0000 |
| 3D-no boost vs IMRT-no boost | 0.1946 | 0.3405 | 1.0000 |
| 3D-no boost vs IMRT-SQB | 0.0985 | 0.2067 | 1.0000 |
| 3D-no boost vs VMAT-no boost | 0.4617 | 0.6464 | 1.0000 |
| 3D-no boost vs VMAT-SIB | 0.2959 | 0.4439 | 1.0000 |
| 3D-no boost vs VMAT-SQB | 0.2181 | 0.3523 | 1.0000 |
| 3D-SQB vs IMRT-no boost | 0.0031 | 0.0312 | 0.0661 * |
| 3D-SQB vs IMRT-SQB | 0.7929 | 0.8824 | 1.0000 |
| 3D-SQB vs VMAT-no boost | 0.0225 | 0.0676 | 0.4733 |
| 3D-SQB vs VMAT-SIB | 0.0059 | 0.0312 | 0.1246 * |
| 3D-SQB vs VMAT-SQB | 0.9411 | 0.9411 | 1.0000 |
| IMRT-no boost vs IMRT-SQB | 0.0031 | 0.0312 | 0.0652 * |
| IMRT-no boost vs VMAT-no boost | 0.6007 | 0.7884 | 1.0000 |
| IMRT-no boost vs VMAT-SIB | 0.7712 | 0.8824 | 1.0000 |
| IMRT-no boost vs VMAT-SQB | 0.0201 | 0.0676 | 0.4214 |
| IMRT-SQB vs VMAT-no boost | 0.0194 | 0.0676 | 0.4081 |
| IMRT-SQB vs VMAT-SIB | 0.0057 | 0.0312 | 0.1206 * |
| IMRT-SQB vs VMAT-SQB | 0.9024 | 0.9411 | 1.0000 |
| VMAT-no boost vs VMAT-SIB | 0.7984 | 0.8824 | 1.0000 |
| VMAT-no boost vs VMAT-SQB | 0.0677 | 0.1579 | 0.8219 |
| VMAT-SIB vs VMAT-SQB | 0.0330 | 0.0867 | 0.6937 |

**Table 4.6:** Raw and corrected p-values from the Post-hoc Dunn test for Item 25_1. An asterisk indicates a significant result under the Benjamini-Hochberg correction, and two asterisks indicate a significant result under the Bonferroni correction.

### 4.3.2 Itching (28_1)

In figure 4.7 the baseline for itching (item 28_1) is displayed. The proportion of patients reporting no itching varied between groups, ranging from 57%, in the IMRT-SQB group, to 73%, in the VMAT-SIB group. Across all the groups mild itching (score=2) was reported between 15%–26%, with VMAT-SQB reporting the lowest percentage and IMRT-no boost group the highest. Taken together, baseline scores of 1 and 2 represented between 80% and 90% of patients in each treatment group. Overall the only significant difference between groups could be found between IMRT-SQB and VMAT-no boost, were the severity before the radiotherapy treatment was significantly higher in the IMRT-SQB group.

In general, the percentage of patients who reported itching (scores 2–5) after the final treatment increased compared to baseline. For the VMAT-no boost group, the percentage of patients who reported no itching remained above 50%. The increase was especially strong for the VMAT-SQB group, where the percentage for experiencing itching increased from 27% to 67%. The changes from baseline after the treatment for itching were stronger than those for skin dryness (25_1).

The groups with the least severe itching were all no-boost groups and VMAT-SIB. The VMAT-SIB distribution was very similar to the IMRT-no boost distribution, with a maximum difference of 2.5 in the percentages of the scores. No significant differences were observed between any combinations of these four groups from the Post-hoc Dunn test. The results of the statistical tests are listed in table 4.7.

More severe itching scores were observed in all SQB groups. Statistically significant differences were found, when comparing the 3D-no boost group with both the 3D-SQB and the IMRT-SQB. Further significant differences were observed when comparing the VMAT-SIB group with the 3D-SQB and IMRT-SQB. All reported differences remained significant after applying the Bonferroni correction.

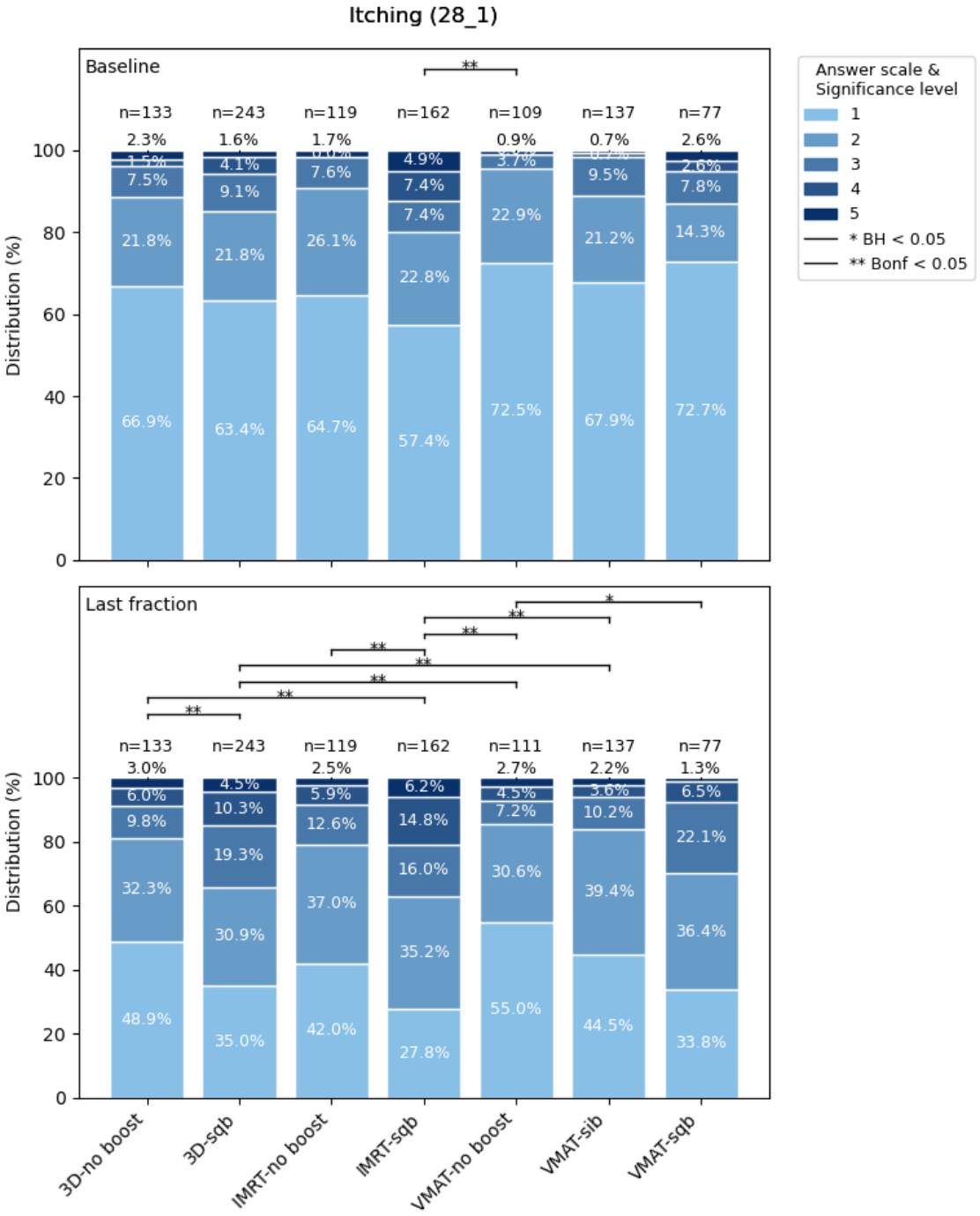


**Figure 4.7:** Normalized PRO frequencies for Item 28_1 at baseline and after treatment. Brackets above the histograms connect groups with significant differences after correction.

| Compared techniques | Raw p | BH p | Bonf p |
|---|---|---|---|
| 3D-no boost vs 3D-SQB | 0.0011 | 0.0039 | 0.0233 ** |
| 3D-no boost vs IMRT-no boost | 0.3870 | 0.4515 | 1.0000 |
| 3D-no boost vs IMRT-SQB | <0.0001 | 0.0002 | 0.0003 ** |
| 3D-no boost vs VMAT-no boost | 0.3137 | 0.3875 | 1.0000 |
| 3D-no boost vs VMAT-SIB | 0.8693 | 0.8693 | 1.0000 |
| 3D-no boost vs VMAT-SQB | 0.0396 | 0.0832 | 0.8320 |
| 3D-SQB vs IMRT-no boost | 0.0302 | 0.0704 | 0.6332 |
| 3D-SQB vs IMRT-SQB | 0.1338 | 0.2007 | 1.0000 |
| 3D-SQB vs VMAT-no boost | <0.0001 | 0.0002 | 0.0006 ** |
| 3D-SQB vs VMAT-SIB | 0.0019 | 0.0057 | 0.0400 ** |
| 3D-SQB vs VMAT-SQB | 0.6626 | 0.6957 | 1.0000 |
| IMRT-no boost vs IMRT-SQB | 0.0011 | 0.0039 | 0.0227 ** |
| IMRT-no boost vs VMAT-no boost | 0.0705 | 0.1233 | 1.0000 |
| IMRT-no boost vs VMAT-SIB | 0.4769 | 0.5271 | 1.0000 |
| IMRT-no boost vs VMAT-SQB | 0.2047 | 0.2865 | 1.0000 |
| IMRT-SQB vs VMAT-no boost | <0.0001 | <0.0001 | <0.0001 ** |
| IMRT-SQB vs VMAT-SIB | <0.0001 | 0.0002 | 0.0006 ** |
| IMRT-SQB vs VMAT-SQB | 0.1308 | 0.2007 | 1.0000 |
| VMAT-no boost vs VMAT-SIB | 0.2416 | 0.3170 | 1.0000 |
| VMAT-no boost vs VMAT-SQB | 0.0042 | 0.0111 | 0.0889 * |
| VMAT-SIB vs VMAT-SQB | 0.0538 | 0.1028 | 1.0000 |

**Table 4.7:** Raw and corrected p-values from the Post-hoc Dunn test for Item 28_1. An asterisk indicates a significant result under the Benjamini-Hochberg correction, and two asterisks indicate a significant result under the Bonferroni correction.

### 4.3.3 Radiation skin reaction (36_2)

At baseline, almost all scores fell into the categories "not at all" (score 1) or "moderate" (score 3), as shown in figure 4.8. The proportion reporting score 1 ranged from 73% to 81% across groups before treatment, with no statistically significant differences observed between them.

Following completion of treatment, the PRO score distribution changed a lot compared to baseline (figure 4.8) and all score levels (1–5) were represented to a non-negligible extent. The proportion of patients reporting no radiation skin reaction decreased from 70%–80% at baseline to a maximum of 30% post-treatment, and for the IMRT-SQB group, only 11% remained in this category. Scores 2 (mild) and 3 (moderate) together accounted for more than half of the patient responses in all groups. The highest percentages of very severe side effects were observed in the SQB groups, where 6%–8% of

patients reported the maximum score. Further statistically significant differences between the groups were observed for 8 group pairings after treatment completion.

| Compared techniques | Raw p | BH p | Bonf p |
|---|---|---|---|
| 3D-no boost vs 3D-SQB | <0.0001 | 0.0001 | 0.0004** |
| 3D-no boost vs IMRT-no boost | 0.0830 | 0.1225 | 1.0000 |
| 3D-no boost vs IMRT-SQB | <0.0001 | <0.0001 | <0.0001 ** |
| 3D-no boost vs VMAT-no boost | 0.5372 | 0.6267 | 1.0000 |
| 3D-no boost vs VMAT-SIB | 0.0627 | 0.1013 | 1.0000 |
| 3D-no boost vs VMAT-SQB | 0.0875 | 0.1225 | 1.0000 |
| 3D-SQB vs IMRT-no boost | 0.0295 | 0.0516 | 0.6191 |
| 3D-SQB vs IMRT-SQB | 0.2213 | 0.2733 | 1.0000 |
| 3D-SQB vs VMAT-no boost | <0.0001 | <0.0001 | <0.0001** |
| 3D-SQB vs VMAT-SIB | 0.0273 | 0.0516 | 0.5741 |
| 3D-SQB vs VMAT-SQB | 0.0961 | 0.1261 | 1.0000 |
| IMRT-no boost vs IMRT-SQB | 0.0023 | 0.0081 | 0.0489 ** |
| IMRT-no boost vs VMAT-no boost | 0.0239 | 0.0516 | 0.5016 |
| IMRT-no boost vs VMAT-SIB | 0.9503 | 0.9503 | 1.0000 |
| IMRT-no boost vs VMAT-SQB | 0.8592 | 0.9436 | 1.0000 |
| IMRT-SQB vs VMAT-no boost | <0.0001 | <0.0001 | <0.0001** |
| IMRT-SQB vs VMAT-SIB | 0.0019 | 0.0081 | 0.0406 * |
| IMRT-SQB vs VMAT-SQB | 0.0136 | 0.0407 | 0.2849 * |
| VMAT-no boost vs VMAT-SIB | 0.0166 | 0.0436 | 0.3486 * |
| VMAT-no boost vs VMAT-SQB | 0.0289 | 0.0516 | 0.6069 |
| VMAT-SIB vs VMAT-SQB | 0.8987 | 0.9436 | 1.0000 |

**Table 4.8:** Raw and corrected p-values from the Post-hoc Dunn test for Item 36_2. An asterisk indicates a significant result under the Benjamini-Hochberg correction, and two asterisks indicate a significant result under the Bonferroni correction.

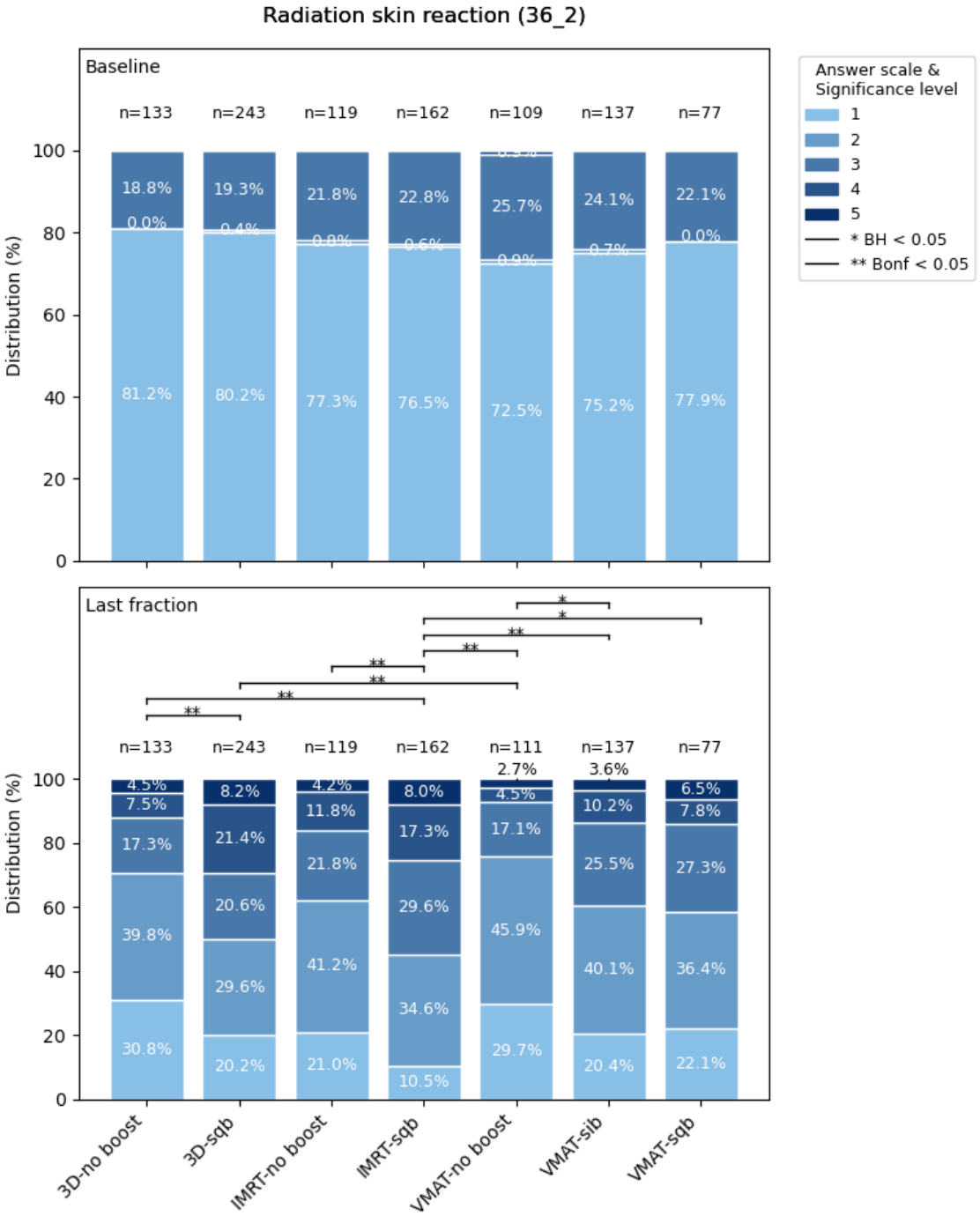


**Figure 4.8:** Normalized PRO frequencies for Item 36_2 at baseline and after treatment. Brackets above the histograms connect groups with significant differences after correction.

### 4.3.4 Skin darkening (37_1)

Figure 4.8 shows the baseline of the PRO for skin darkening. This item is unique because the answer metric was binary: whether or not patients observed unusual darkening of their skin. Before radiotherapy, nearly all patients reported that they did not observe skin darkening. Across all groups, the highest percentage for "yes" (score = 2) was 4% for the VMAT-SQB group. In the IMRT-no boost group all patients reported no skin darkening. Similar to question 36_2 (radiation reaction), no significant differences were observed at baseline, so all groups were the same.

After completion of radiotherapy, the PRO scores changed, as shown in figure 4.8. Skin darkening was reported by 24%–49% of patients in the groups. The groups that reported the lowest proportion of skin darkening were VMAT-no boost, 3D-no boost, and VMAT-SIB, with less than 30% reporting skin darkening. The IMRT-no boost group reported a slightly higher percentage, with 35% reporting skin darkening. However, there were no statistically significant differences between the four groups.

In the remaining three groups, all of which were SQB groups, skin darkening was observed more often, with 45%–55% of patients reported the side effect. Excluding VMAT-SQB, significant differences were observed in each pairing between the four lower skin darkening groups and the two remaining SQB groups. This means that skin darkening occurred more frequently in patients treated with SQB than those treated with SIB or without a boost.

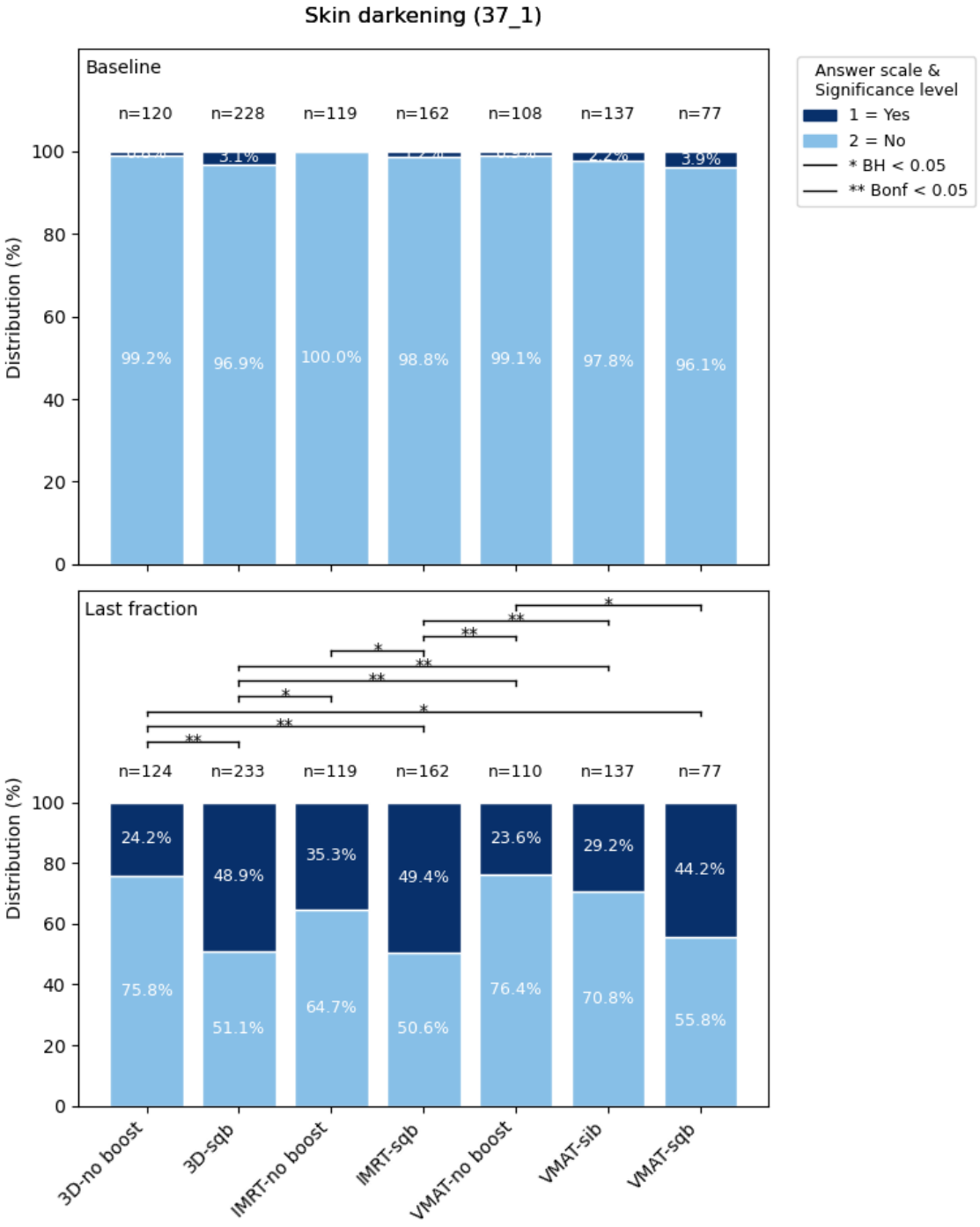


**Figure 4.9:** Normalized PRO frequencies for Item 37_1 at baseline and after treatment. Brackets above the histograms connect groups with significant differences after correction.

| Compared techniques | Raw p | BH p | Bonf p |
|---|---|---|---|
| 3D-no boost vs 3D-SQB | <0.0001 | 0.0001 | <0.0001** |
| 3D-no boost vs IMRT-no boost | 0.0749 | 0.1211 | 1.0000 |
| 3D-no boost vs IMRT-SQB | <0.0001 | <0.0001 | <0.0003** |
| 3D-no boost vs VMAT-no boost | 0.9302 | 0.9302 | 1.0000 |
| 3D-no boost vs VMAT-SIB | 0.4060 | 0.5015 | 1.0000 |
| 3D-no boost vs VMAT-SQB | 0.0046 | 0.0121 | 0.0970 * |
| 3D-SQB vs IMRT-no boost | 0.0127 | 0.0297 | 0.2676 * |
| 3D-SQB vs IMRT-SQB | 0.9269 | 0.9302 | 1.0000 |
| 3D-SQB vs VMAT-no boost | <0.0001 | 0.0001 | 0.0001 ** |
| 3D-SQB vs VMAT-SIB | 0.0002 | 0.0007 | 0.0034 ** |
| 3D-SQB vs VMAT-SQB | 0.4549 | 0.5028 | 1.0000 |
| IMRT-no boost vs IMRT-SQB | 0.0163 | 0.0342 | 0.3421 * |
| IMRT-no boost vs VMAT-no boost | 0.0696 | 0.1211 | 1.0000 |
| IMRT-no boost vs VMAT-SIB | 0.3165 | 0.4431 | 1.0000 |
| IMRT-no boost vs VMAT-SQB | 0.2123 | 0.3184 | 1.0000 |
| IMRT-SQB vs VMAT-no boost | <0.0001 | <0.0001 | 0.0004 ** |
| IMRT-SQB vs VMAT-SIB | 0.0003 | 0.0012 | 0.0072 ** |
| IMRT-SQB vs VMAT-SQB | 0.4369 | 0.5028 | 1.0000 |
| VMAT-no boost vs VMAT-SIB | 0.3712 | 0.4872 | 1.0000 |
| VMAT-no boost vs VMAT-SQB | 0.0045 | 0.0121 | 0.0939 * |
| VMAT-SIB vs VMAT-SQB | 0.0306 | 0.0584 | 0.6428 |

**Table 4.9:** Raw and corrected p-values from the Post-hoc Dunn test for Item 37_1. An asterisk indicates a significant result under the Benjamini-Hochberg correction, and two asterisks indicate a significant result under the Bonferroni correction.

### 4.3.5 Breast swelling and tenderness (72_1)

Before the first radiotherapy treatment, the majority of patients reported no swelling or tenderness in the breast. Over 50% of patients in each group reported a score of 1, as can be seen in figure 4.10. Higher severity scores (3-5) combined reached a maximum of 10% among all groups. No significant differences were observed at baseline.

Figure 4.10 shows that the severity of breast swelling and tenderness changed after the last treatment. Compared to baseline, when over half of the patients in each group reported no swelling or tenderness, the percentage of score 1 fell below 40% for all groups. By the last treatment, the most common score was 2 (mild). Reports of higher severity scores (3–5) increased from a maximum of 10% at baseline to over 20% across all groups.

The group with the highest proportion of patients who reported a score of 1 after treat-

ment was the VMAT-no boost group, at 39%, followed closely by the 3D-no boost group, at 38%. The group in which the most patients experienced swelling and tenderness to some degree (scores 2–5) was the IMRT-SQB group, with only 24% reporting a score of 1.

Compared to the previous two items, there are fewer significant differences between the groups, only four cases. One significant difference to point out is between the 3D-no boost and 3D-SQB, where swelling was reported as more severe for the SBQ treatment.

| Compared techniques | Raw p | BH p | Bonf p |
|---|---|---|---|
| 3D-no boost vs 3D-SQB | 0.0041 | 0.0216 | 0.0862 * |
| 3D-no boost vs IMRT-no boost | 0.3017 | 0.4084 | 1.0000 |
| 3D-no boost vs IMRT-SQB | 0.0009 | 0.0093 | 0.0186 ** |
| 3D-no boost vs VMAT-no boost | 0.8451 | 0.8874 | 1.0000 |
| 3D-no boost vs VMAT-SIB | 0.1083 | 0.2293 | 1.0000 |
| 3D-no boost vs VMAT-SQB | 0.3112 | 0.4084 | 1.0000 |
| 3D-SQB vs IMRT-no boost | 0.1092 | 0.2293 | 1.0000 |
| 3D-SQB vs IMRT-SQB | 0.4333 | 0.5353 | 1.0000 |
| 3D-SQB vs VMAT-no boost | 0.0035 | 0.0216 | 0.0732 * |
| 3D-SQB vs VMAT-SIB | 0.2858 | 0.4084 | 1.0000 |
| 3D-SQB vs VMAT-SQB | 0.2084 | 0.3978 | 1.0000 |
| IMRT-no boost vs IMRT-SQB | 0.0321 | 0.1350 | 0.6749 |
| IMRT-no boost vs VMAT-no boost | 0.2388 | 0.4059 | 1.0000 |
| IMRT-no boost vs VMAT-SIB | 0.6030 | 0.7035 | 1.0000 |
| IMRT-no boost vs VMAT-SQB | 0.9199 | 0.9199 | 1.0000 |
| IMRT-SQB vs VMAT-no boost | 0.0008 | 0.0093 | 0.0163 ** |
| IMRT-SQB vs VMAT-SIB | 0.0955 | 0.2293 | 1.0000 |
| IMRT-SQB vs VMAT-SQB | 0.0780 | 0.2293 | 1.0000 |
| VMAT-no boost vs VMAT-SIB | 0.0841 | 0.2293 | 1.0000 |
| VMAT-no boost vs VMAT-SQB | 0.2513 | 0.4059 | 1.0000 |
| VMAT-SIB vs VMAT-SQB | 0.7231 | 0.7992 | 1.0000 |

**Table 4.10:** Raw and corrected p-values from the Post-hoc Dunn test for Item 72_1. An asterisk indicates a significant result under the Benjamini-Hochberg correction, and two asterisks indicate a significant result under the Bonferroni correction.

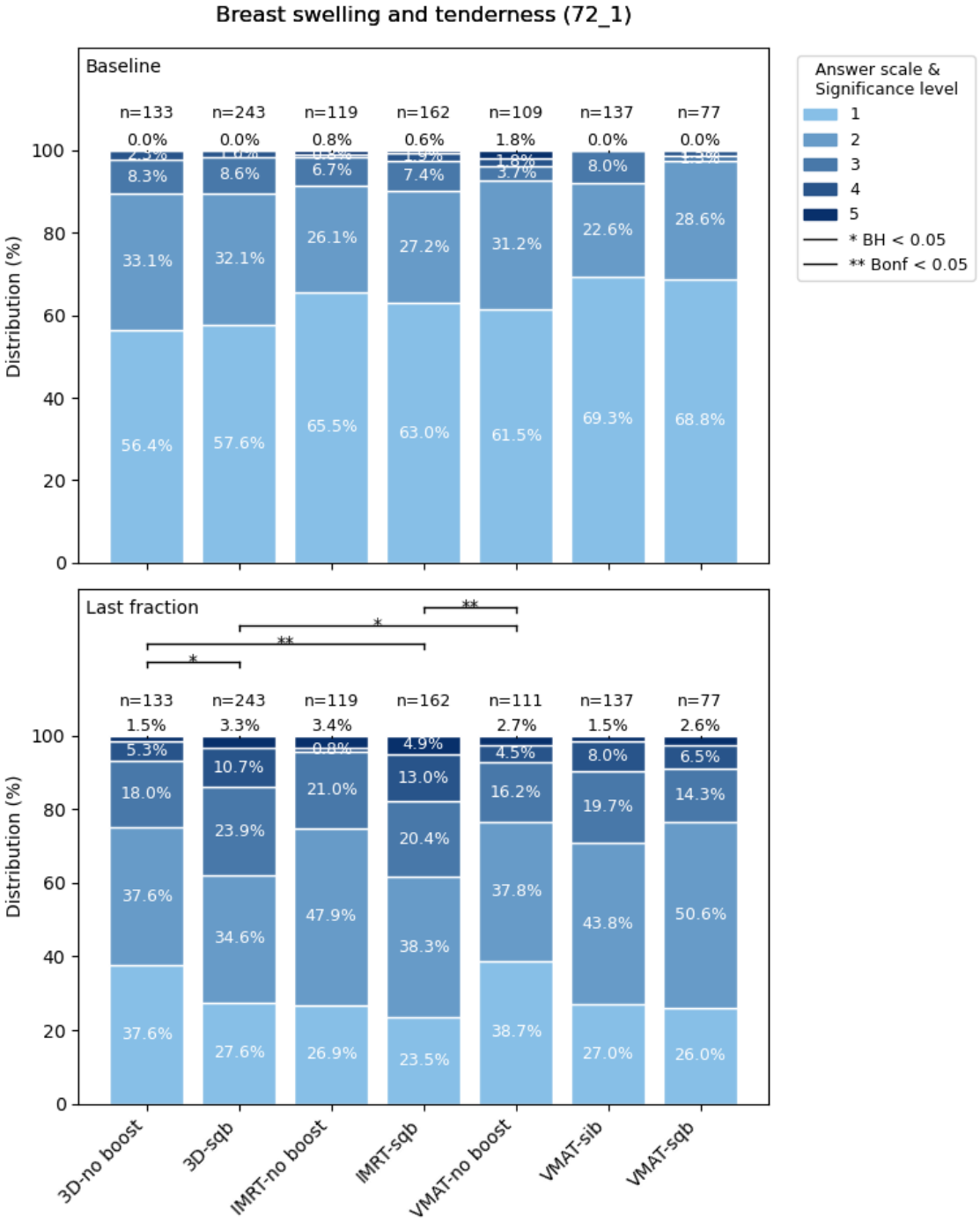


**Figure 4.10:** Normalized PRO frequencies for Item 72_1 at baseline and after treatment. Brackets above the histograms connect groups with significant differences after correction.

## 4.4 Experiment 2: Correlation between acute PRO and dose-volume parameter

To determine the typical skin doses, the skin volumes irradiated with 10 Gy, 20 Gy, 30 Gy, and 40 Gy were compared for the combination of treatment techniques and boost methods. The distribution of skin volumes is illustrated using violin plots, where the width of the plot represents the frequency of observations. As the plots in figure 4.11 show, the irradiated skin volume for the low-dose of 10 Gy were similar for 3D-CRT and IMRT techniques with the mean volumes ranging between 72 ($\pm$31) cm$^3$–93 ($\pm$25) cm$^3$. However, higher irradiated skin volumes were observed in the VMAT groups with mean volumes over 100 cm$^3$. In the medium dose ranges of 20 Gy and 30 Gy, little differences were observed between the groups. However, in the high-dose range of 40 Gy, higher irradiated skin volumes were seen for the patients who received a boost dose. Patients with larger irradiated skin volumes were observed for the SQB compared to the SIB treatment plans. It should be noted however, that the IMRT-SIB group was much smaller, with only 36 patients. All mean skin volumes are displayed in table 4.11

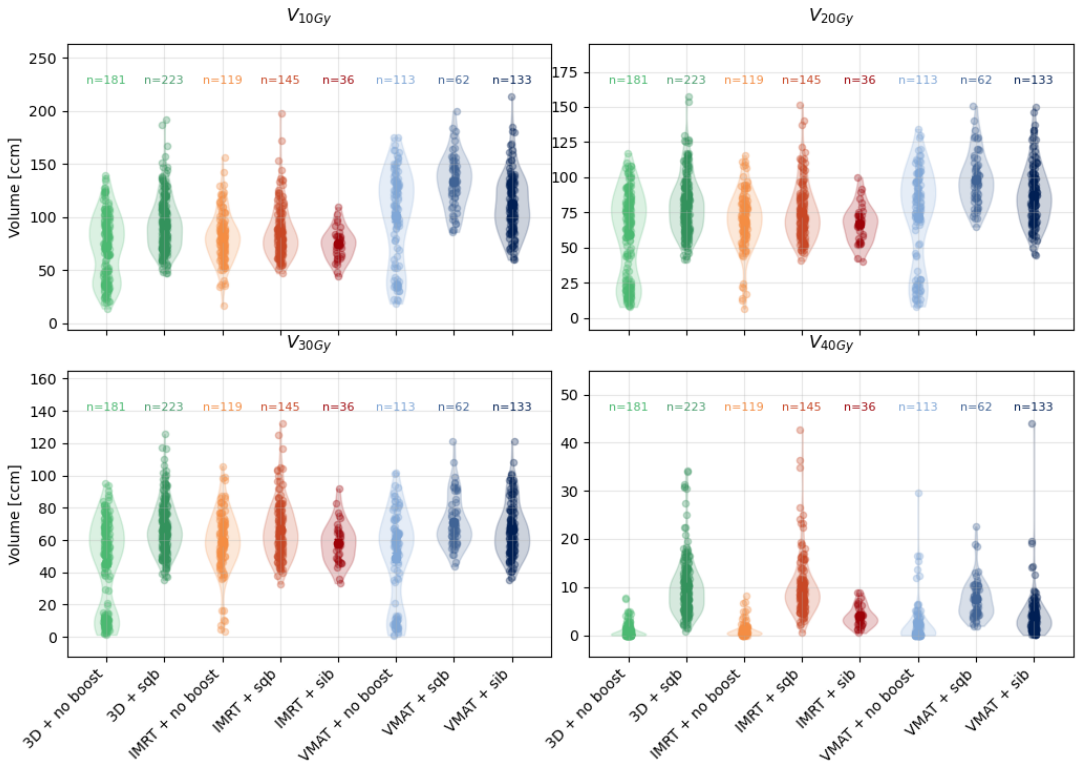


**Figure 4.11:** Skin dose volumes for all treatment technique-boost method groups ranging from $V_{10\text{Gy}}$–$V_{40\text{Gy}}$.

| | $V_{10Gy}$ [cm$^3$] | | $V_{20Gy}$ [cm$^3$] | | $V_{30Gy}$ [cm$^3$] | | $V_{40Gy}$ [cm$^3$] | |
|---|---|---|---|---|---|---|---|---|
| Technique - boost | Mean | SD | Mean | SD | Mean | SD | Mean | SD |
| 3D-no boost | 72.1 | 30.6 | 59.4 | 30.4 | 45.6 | 27.1 | 0.9 | 1.3 |
| 3D-SQB | 93.1 | 25.3 | 80.5 | 20.3 | 67.5 | 15.9 | 10.0 | 5.8 |
| IMRT-no boost | 80.9 | 23.3 | 69.5 | 20.6 | 59.1 | 18.9 | 1.0 | 1.5 |
| IMRT-SQB | 86.2 | 24.6 | 75.5 | 20.1 | 66.7 | 17.4 | 10.2 | 6.3 |
| IMRT-SIB | 74.6 | 14.9 | 66.9 | 13.4 | 58.3 | 12.7 | 4.0 | 2.2 |
| VMAT-no boost | 100.2 | 43.2 | 71.6 | 34.8 | 49.3 | 28.1 | 2.2 | 4.3 |
| VMAT-SQB | 133.5 | 25.2 | 98.3 | 18.5 | 70.9 | 15.8 | 7.5 | 4.1 |
| VMAT-SIB | 112.3 | 28.4 | 87.5 | 21.1 | 66.4 | 16.5 | 4.1 | 4.8 |

**Table 4.11:** Mean skin volumes of treatment technique-boost method.

$V_{40Gy}$ was selected for further analysis to evaluate its impact on worsening events of side effects, as high-dose volumes have been selected as metrics for investigation of skin side effects in the literature [45] [46]. Spearman's correlation analysis revealed the strongest association between side effect severity and skin volume receiving 40 Gy ($V_{40Gy}$), although the correlations were weak, with correlation coefficients ranging from 0.14–0.24 (see table 4.12).

| | 25_1 | | 28_1 | | 36_2 | | 37_1 | | 72_1 | |
|---|---|---|---|---|---|---|---|---|---|---|
| | $\rho$ | p | $\rho$ | p | $\rho$ | p | $\rho$ | p | $\rho$ | p |
| $V_{10Gy}$ | 0.073 | 0.020 | 0.022 | 0.481 | 0.137 | <0.001 | 0.112 | <0.001 | 0.074 | 0.017 |
| $V_{20Gy}$ | 0.087 | 0.005 | 0.044 | 0.159 | 0.175 | <0.001 | 0.133 | <0.001 | 0.090 | 0.004 |
| $V_{30Gy}$ | 0.112 | <0.001 | 0.074 | 0.017 | 0.238 | <0.001 | 0.167 | <0.001 | 0.115 | <0.001 |
| $V_{40Gy}$ | 0.138 | <0.001 | 0.187 | <0.001 | 0.243 | <0.001 | 0.184 | <0.001 | 0.140 | <0.001 |

**Table 4.12:** Spearman's correlation between radiation-induced skin toxicities and $V_{10Gy}$, $V_{20Gy}$, $V_{30Gy}$, and $V_{40Gy}$. The highest correlation factors $\rho$ between the dose level and item score is marked in blue

The cohort sizes varied between 920 and 1,031 patients across the different PRO items. A larger number of patients were excluded from 25_1 due to baseline scores of 4 (severe) or 5 (very severe) (see previous results chapter on skin dryness). As the table 4.13 shows, the number of events with a difference of two or more was less compared to events defined with having a difference of one or more. For $\Delta \geq 2$ the observed events were 28%–38% of the events for $\Delta \geq 1$.

| | Events for $\Delta \geq 1$ | Events for $\Delta \geq 2$ | Cohort size |
|---|---|---|---|
| 25_1 | 322 | 91 | 920 |
| 28_1 | 410 | 156 | 979 |
| 36_2 | 636 | 318 | 1031 |
| 37_1 | 355 | - | 1000 |
| 72_1 | 518 | 174 | 1013 |

**Table 4.13:** Number of events depending on the event definition.

In general, the volume of skin receiving 40 Gy was consistently associated with a higher likelihood of worsening of acute side effects, as odds ratios were greater than 1 for all items. As can be seen from figure 4.12, this was significant for the following three items: itching (28_1), radiation skin reaction (36_2), and skin darkening (37_1). The odds ratio for these three items ranged between 1.055–1.060, meaning the risk of worsening events increased by 5.5%–6%, respectively, for every additional 1 $cm^3$ of $V_{40Gy}$. No significant association between $V_{40Gy}$ could be detected for breast swelling with $\Delta \geq 2$. However, it was significant for the less strict event definition with $\Delta \geq 1$.

Age was a significant covariate for all PRO items. However, in contrast to the irradiated skin volume, the odds ratio was always less than one. Meaning that older patients reported less acute worsening of skin side effects.
All other clinical factors, including surgery, chemotherapy, hormone therapy, and laterality, showed no significant association with any of the PRO items. The data for the logistic regression are shown in table 4.14

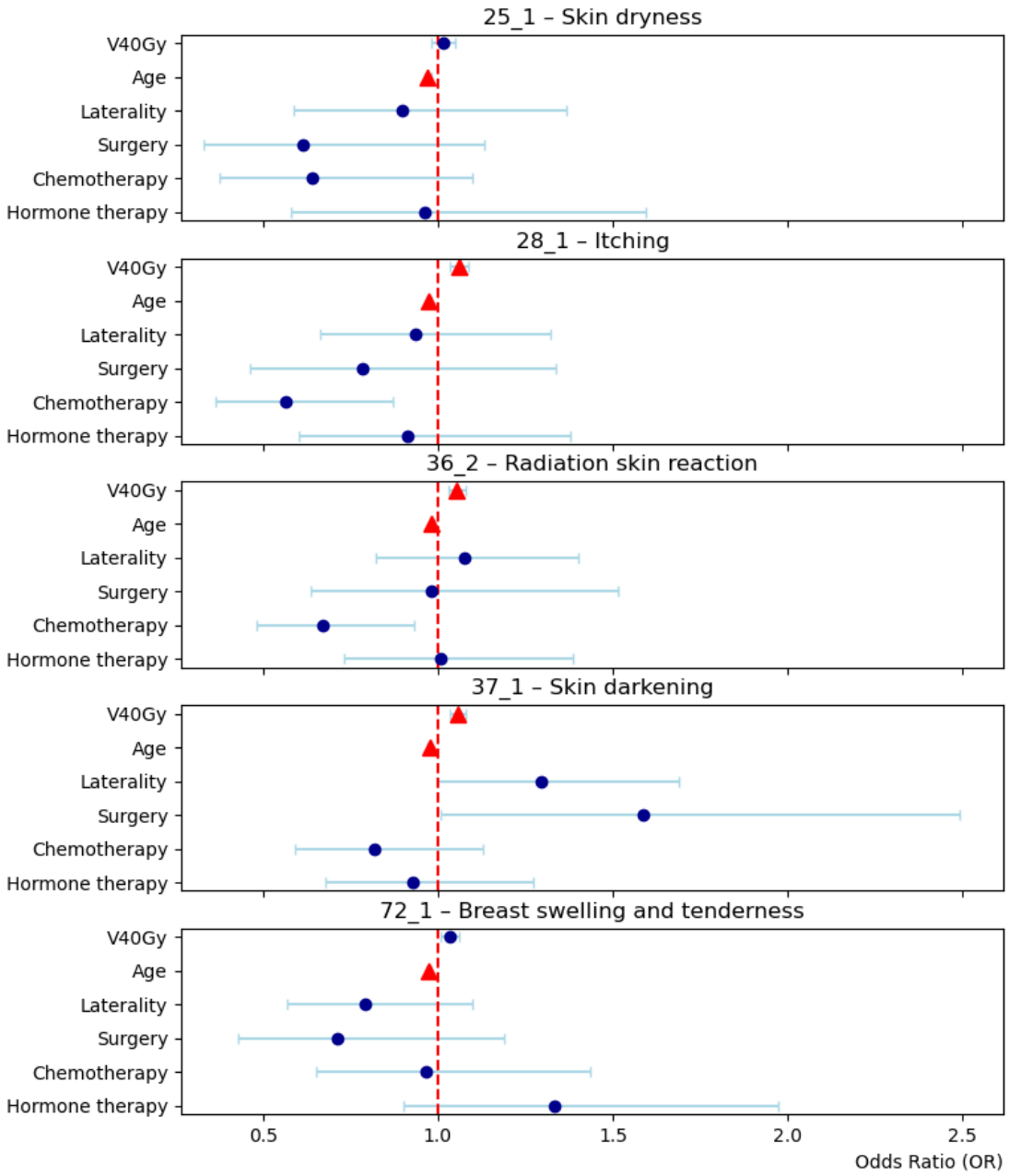


**Figure 4.12:** Odds ratio including confidence intervals (95%) of the predictors for each of the five skin side effects items. Red triangles indicate significant predictors.

| | OR | 2.5% | 97.5% | p | OR | 2.5% | 97.5% | p |
|---|---|---|---|---|---|---|---|---|
| | 25_1 | | | | 28_1 | | | |
| $V_{40Gy}$ | 1.016 | 0.981 | 0.022 | 0.378 | 1.060 | 1.033 | 1.088 | **<0.001** |
| Age | 0.971 | 0.962 | 0.981 | **<0.001** | 0.973 | 0.965 | 0.981 | **<0.001** |
| Hormone therapy | 0.961 | 0.579 | 1.595 | 0.878 | 0.913 | 0.605 | 1.379 | 0.666 |
| Chemo therapy | 0.641 | 0.375 | 1.098 | 0.105 | 0.565 | 0.367 | 0.870 | 0.010 |
| Surgery | 0.614 | 0.333 | 1.132 | 0.118 | 0.786 | 0.462 | 1.337 | 0.374 |
| Laterality | 0.897 | 0.588 | 1.367 | 0.612 | 0.935 | 0.663 | 1.320 | 0.704 |
| | 36_2 | | | | 37_1 | | | |
| $V_{40Gy}$ | 1.055 | 1.031 | 1.079 | **<0.001** | 1.057 | 1.033 | 1.081 | **<0.001** |
| Age | 0.983 | 0.976 | 0.989 | **<0.001** | 0.976 | 0.970 | 0.983 | **<0.001** |
| Hormone therapy | 1.008 | 0.733 | 1.386 | 0.961 | 0.929 | 0.679 | 1.271 | 0.646 |
| Chemo therapy | 0.671 | 0.482 | 0.933 | 0.018 | 0.818 | 0.593 | 1.130 | 0.223 |
| Surgery | 0.981 | 0.636 | 1.514 | 0.932 | 1.585 | 1.008 | 2.492 | 0.046 |
| Laterality | 1.074 | 0.823 | 1.402 | 0.597 | 1.297 | 0.995 | 1.689 | 0.054 |
| | 72_1 | | | | | | | |
| $V_{40Gy}$ | 1.033 | 1.006 | 1.060 | 0.015 | | | | |
| Age | 0.973 | 0.966 | 0.981 | **<0.001** | | | | |
| Hormone therapy | 1.333 | 0.900 | 1.974 | 0.151 | | | | |
| Chemo therapy | 0.968 | 0.652 | 1.437 | 0.871 | | | | |
| Surgery | 0.713 | 0.428 | 1.190 | 0.196 | | | | |
| Laterality | 0.791 | 0.570 | 1.097 | 0.161 | | | | |

**Table 4.14:** Analysis results of logistic regression. Significant p-values are formatted bold.

## 4.5 Experiment 3: Long-term side effects

Patient responses from the PRO survey were almost complete at baseline and after treatment completion, with only 2 missed responses at baseline. These two patient were excluded for the analysis, since no baseline comparison was possible. The largest dropout occurred at the three-month time point, with more than one-third of patients stopping to fill out the survey at any later time point. This was partly because follow-up responses after treatment completions were not collected until November 2021.
From 3 to 12 months, the response rate remained stable, though some patients missed interim survey responses. The number of responses was higher at 9 months with 561 than it was at 6 months with 548. At the 24 month follow-up however, the response rate dropped strongly due to a large number of patients who had not reached the two-year follow-up point after treatment at the time of data collection on August 18$^{th}$ 2025. Patients who dropped or were pending were right censored in the Cox proportional hazards analysis.

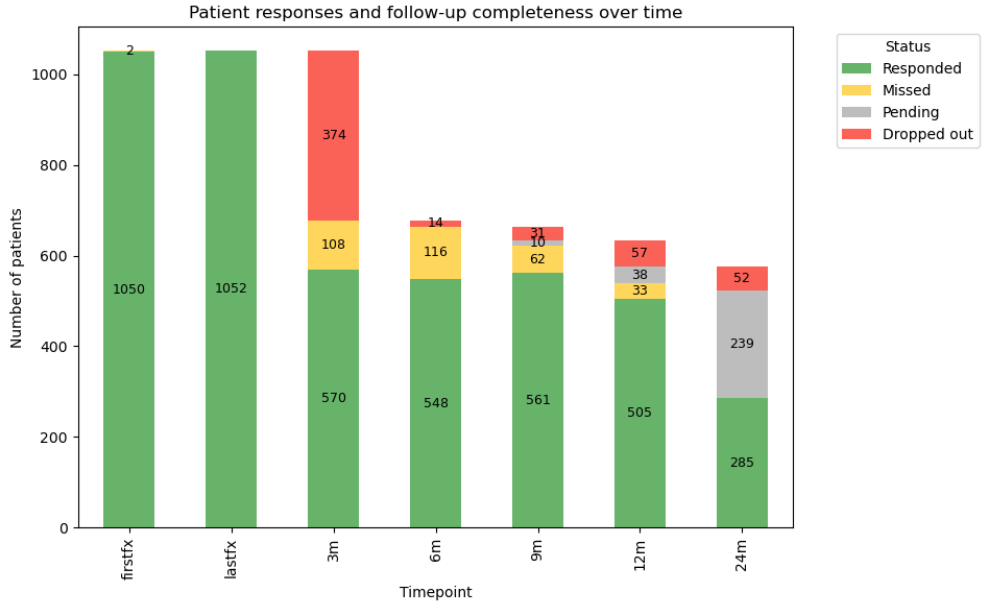


**Figure 4.13:** Number of PRO responses over time. A "Missed" response is categorized, when a patient missed one or more follow-ups, but responded at a later time. The status "Pending" was classified when a patient had not reached the specified time point after treatment. "Drop outs" did not respond at any later time and are displayed at the time of withdrawal. They are excluded from further follow-up statistics.

The Cox proportional hazards model did not reveal any influence of $V_{40\text{Gy}}$ on the worsening of long-term side effects. Further, with the exception of age for two items and the laterality for one item, all other predictors (hormone therapy, chemotherapy and prior surgery) were not significant. Age was significant in the following two items: 37_1 skin darkening and 72_1 breast swelling and tenderness both with hazard ratios smaller than 1, indicating a reduced risk of skin toxicity worsening for late effects with older age. Laterality was a significant predictor for 36_2 (radiation skin reaction) with a hazard ratio of 0.54, indicating a protective effect of sunburn like changes for left sided treatment. The results of the predictors are shown in table 4.15 and visually displayed in figure 4.14.

The probability of complication-free survival from long-term skin side effects decreased for all items at each follow-up period. Overall, the probability of no worsening from baseline after two years was between 85% and 93%, where the highest probability was observed for itching and the lowest corresponded to breast swelling and tenderness. The

| | HR | 2.5% | 97.5% | p | HR | 2.5% | 97.5% | p |
|---|---|---|---|---|---|---|---|---|
| | | | 25_1 | | | | 28_1 | |
| $V_{40Gy}$ | 1.01 | 0.98 | 1.04 | 0.415 | 1.01 | 0.98 | 1.05 | 0.486 |
| Age | 0.98 | 0.96 | 1.00 | 0.016 | 0.98 | 0.96 | 0.99 | 0.014 |
| Hormone therapy | 1.13 | 0.71 | 1.79 | 0.602 | 1.42 | 0.81 | 2.48 | 0.224 |
| Chemo therapy | 0.82 | 0.52 | 1.31 | 0.409 | 0.92 | 0.54 | 1.59 | 0.775 |
| Surgery | 1.10 | 0.58 | 2.10 | 0.772 | 0.92 | 0.43 | 1.94 | 0.822 |
| Laterality | 1.05 | 0.72 | 1.53 | 0.786 | 0.81 | 0.52 | 1.27 | 0.360 |
| | | | 36_2 | | | | 37_1 | |
| $V_{40Gy}$ | 1.02 | 0.99 | 1.05 | 0.181 | 0.98 | 0.95 | 1.01 | 0.200 |
| Age | 0.99 | 0.98 | 1.01 | 0.445 | 0.96 | 0.94 | 0.97 | **<0.001** |
| Hormone therapy | 1.18 | 0.75 | 1.85 | 0.447 | 1.31 | 0.85 | 2.01 | 0.222 |
| Chemo therapy | 1.05 | 0.67 | 1.65 | 0.836 | 1.23 | 0.81 | 1.88 | 0.335 |
| Surgery | 0.63 | 0.36 | 1.11 | 0.111 | 0.95 | 0.52 | 1.74 | 0.872 |
| Laterality | 0.54 | 0.37 | 0.81 | **0.003** | 0.92 | 0.64 | 1.31 | 0.636 |
| | | | 72_1 | | | | | |
| $V_{40Gy}$ | 1.01 | 0.98 | 1.03 | 0.601 | | | | |
| Age | 0.97 | 0.96 | 0.99 | **<0.001** | | | | |
| Hormone therapy | 0.88 | 0.62 | 1.25 | 0.469 | | | | |
| Chemo therapy | 1.20 | 0.83 | 1.72 | 0.333 | | | | |
| Surgery | 1.17 | 0.68 | 2.02 | 0.567 | | | | |
| Laterality | 0.95 | 0.70 | 1.29 | 0.740 | | | | |

**Table 4.15:** Predictive factors associated with long-term radiation skin reactions.

Kaplan-Meier curves of skin dryness and radiation skin reaction were almost identical, with the difference in probability being less than 1%. The largest drop in the probability of no worsening was observed for breast swelling and tenderness at the six month follow-up. Figure 4.15 shows the Kaplan-Meier curves.

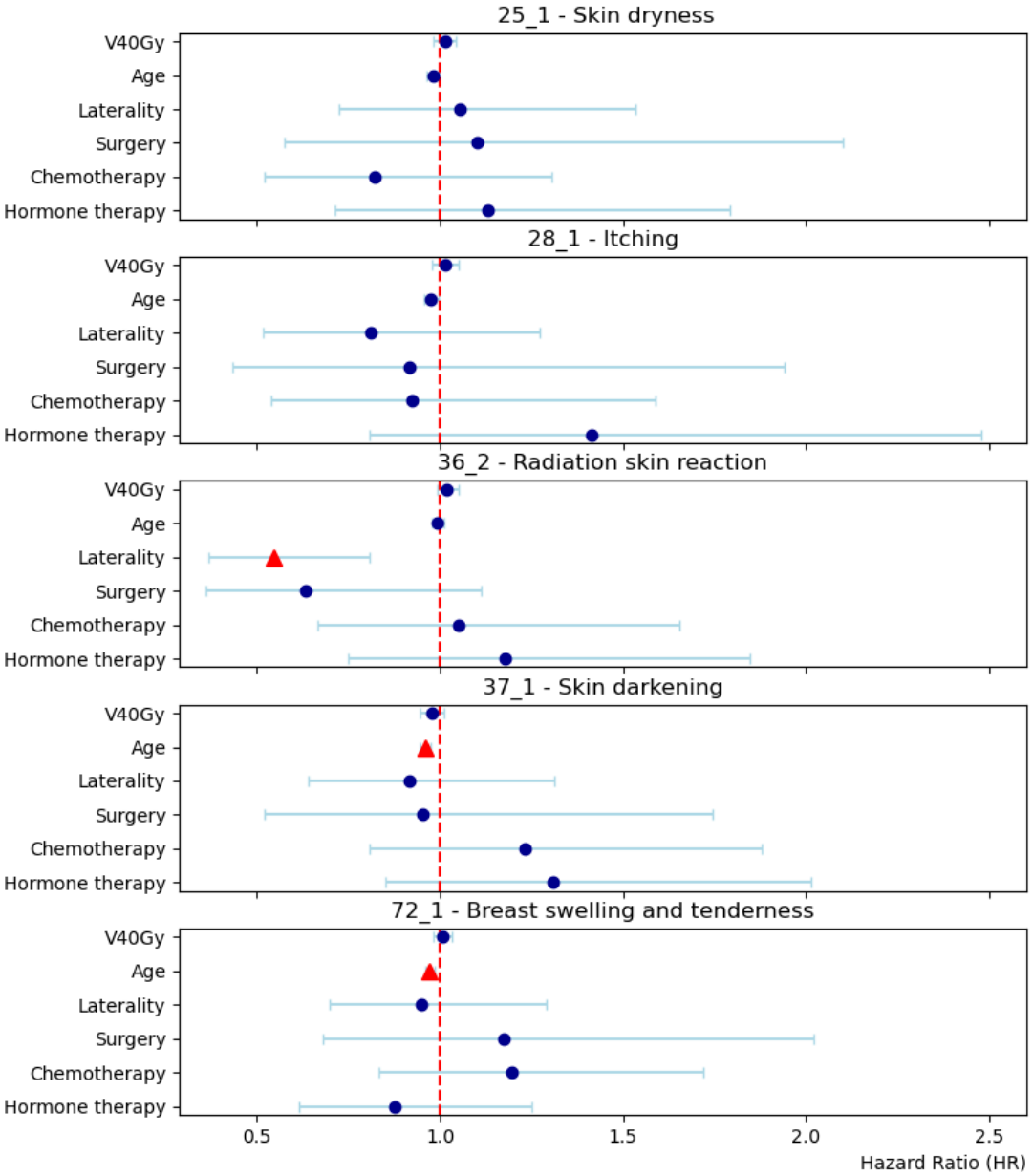


**Figure 4.14:** Hazard ratio including confidence intervals (95%) of the predictors for each of the five skin side effect items. Red triangles indicate significant predictors.

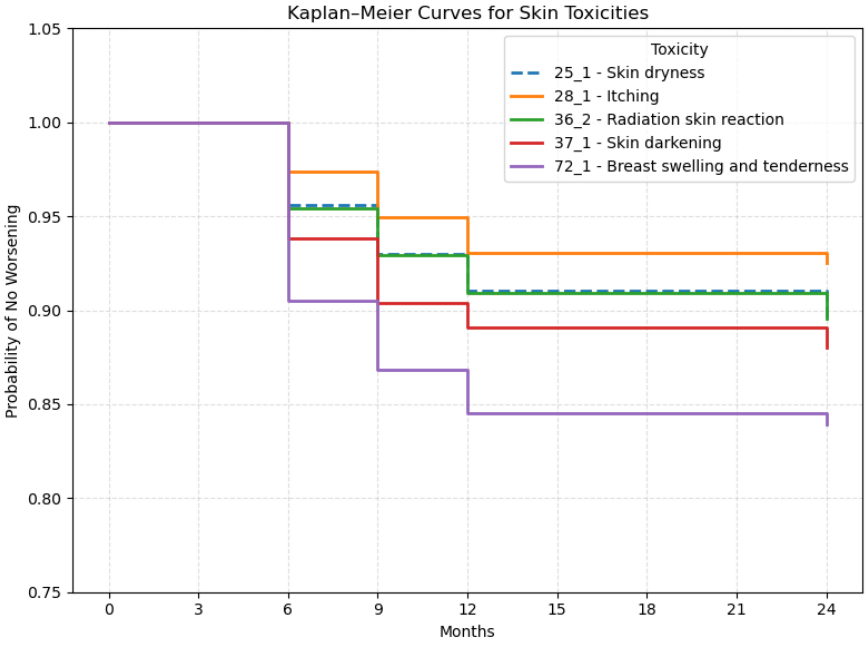


**Figure 4.15:** Probability of no worsening from baseline for long-term side effects. 25_1 was off-set by +0.0005 for better visibly.

# 5 Discussion

The following section discusses the main findings of the three experiments in relation to previous studies. *Experiment 1* compared the severity of radiation-induced side effects of the different treatment techniques and boost methods. *Experiments 2* and *3* focused on the correlation of dose-volume parameters and clinical predictors with worsening events for acute and long-term side effects.

In *Experiment 1* higher mean scores for VMAT-SQB than VMAT-SIB were recorded for 4 of the 5 items, however, no significant difference could be detected. It should be noted that the VMAT-SQB group was smaller than the others, with 77 patients while the other groups ranged between 109–243. This trend was in line with expectations, as previous studies have shown that skin toxicity may be reduced by using SIB rather than SQB [47]. This indicates that switching from SQB to SIB did not result in worsening of skin side effects, despite the higher dose per fraction of the boost volume in the SIB method.
The SIB method represents a more comprehensive planning approach. This may provide better control of dose homogeneity [48] [49], thereby mitigating some of the toxicity despite the higher per-fraction dose. Treatment for SQB patients lasted for one week longer than for patients treated with SIB. The additional week of irradiation meant an extended period of radiation exposure to the skin, which may contribute to higher severity of acute skin reactions.

A shorter radiotherapy treatment duration as in SIB could be beneficial for both patients and clinical workflow. A reduced treatment duration is more convenient for patients because they do not have to come to the clinic as often. This may limit the period during which they experience decreases in quality of life and increases in distress, as these effects have been shown to occur during radiotherapy treatment and returned to baseline levels after completion [50]. From the clinic's perspective, shortening the treatment time by one week can increase the capacity to treat patients.

The PRO baseline severity of skin dryness was much higher than for any other analyzed item. The high baseline combined with significant differences between the treatment technique-boost method groups limited the ability to isolate the effects of radiation therapy on the skin. The elevated baseline might be due to effects of prior treatment, such as chemotherapy, which was received by one third of patients. 30% of chemotherapy was administered adjuvantly, 4–8 weeks prior to radiotherapy.
An increase in patient-reported skin dryness following chemotherapy has been observed

by Kang et al., which persisted up to six months after treatment completion [51] [2]. The study found an association between measured changes of the skin, such as water content, and the reported side effects. The period during which increased dryness was observed overlapped with the time-frame of the radiotherapy in the present study. Therefore, this pre-existing side effects could have influenced the reported acute skin dryness observed during this study and may be one contributing factor to the elevated baseline.

In *Experiment 2* $V_{40\text{Gy}}$ turned out to be a significant predictor for worsening events of acute adverse effects as expected. A larger irradiated high-dose skin volume ($V_{40\text{Gy}}$) increased the probability of experiencing worsening of skin related adverse effects. This could be observed for 3 of the 5 items, namely itching, radiation skin reaction, and skin darkening. When a less strict event definition of worsening of $\Delta \geq 1$ is implemented, $V_{40\text{Gy}}$ was additionally observed as a significant predictor for item 72_1 (breast swelling and tenderness). Compared to the other items, worsening of breast swelling might be a more subtle effect, as the significance was not observed for $\Delta \geq 2$.

In this study the probability of worsening events was reduced with an increase in age. However, the literature on the influence of age on radiotherapy related skin reactions is inconsistent. One study found that younger patients were at higher risk of developing more severe skin reactions [52], while others studies reported no significant association between patient age and acute skin toxicity [53] [54]. In contrast, an increased risk of developing more severe skin side effects with higher age was observed as well [55].

In *Experiment 3* the deaths of patients were not included as this information was not available. Reasons for a drop out of the experiment could be due to death of the patient, which then could be adjusted for in the model.
Contrary to expectation laterality was found to be a significant protective factor of late radiation skin reactions (item 36_2) for left-sided treatment. One possible explanation for this observation might be that left-sided irradiation was administered during deep inspiration breath hold with the aim of reducing the dose to the heart by increasing the distance from the PTV to the heart [56]. In contrast, right-sided irradiation occurred during free breathing. DIBH may therefore have resulted in a closer match between planned and delivered doses, reducing dose hot spots and lowering the risk of side effects. However, it should be noted that this association was observed only for item 36_2, while no effect of laterality was found for all other items in both the acute and late setting.

In this study, no significant association was observed between $V_{40\text{Gy}}$ and long-term

[2] Inconsistencies were observed in the reported percentages of skin dryness when comparing the values presented in the text with those shown in the corresponding table in the cited study. For the purposes of this analysis, the values in the text were assumed to be correct. However, it should be noted that using the values from the table would not change the outcome or interpretation of the findings.

patient-reported skin events. However, previous research has identified similar dose–volume parameters of the skin as predictors of late toxicity. For example, Cichetti et al. [57] found that both $V_{20\mathrm{Gy}}$ (50% of the prescribed dose) and $V_{42\mathrm{Gy}}$ (105%) were independently associated with late adverse skin reactions in a cohort over 1,000 patients.

This analysis used a similar dose-volume parameter, as $V_{40\mathrm{Gy}}$ corresponds to 100% of the prescribed dose for treatment without a boost, 80% with SQB and 83% with an SIB. The absence of the $V_{40\mathrm{Gy}}$ as a significant predictor may therefore be related to the generally mild average acute skin reactions reported by patients, which could have limited the progression to late effects. Additionally a smaller number of long-term events and the loss of follow-ups may have reduced the statistical power to detect subtle associations. It is also possible that medium-dose volumes, such as $V_{20\mathrm{Gy}}$ as reported by DeRose et al. [58], might better reflect the relevant skin exposure. Finally, biological processes after the acute phase might outweigh the initial high-dose volume influence observed for acute reactions.

The doses and corresponding irradiated volumes were based on the treatment plan; however, the actual absorbed doses were not measured. The accuracy to which those match depend on several factors, such as the calculation method used during planning and positioning of the patient. Skin doses are particularly difficult to calculate due to the curved surface on the breast. A tolerance of up to 27% between measured and TPS calculated skin doses have been reported by Court et al. [59]. When comparing measured doses with prescribed ones, the study by Toossi et al. [60] found the skin dose was lower in 81% and higher in 19% at different points on the skin, where hotspots can occur, which could lead to adverse skin reactions. Furthermore, this study focused only on skin dose and related dose effects. While other organs at risk during radiotherapy for breast cancer, such as the heart and lungs were not included in the analysis even though they receive non-negligible radiation exposure during treatment [61].

Further this study relied on PROs only, and no clinical grading was assessed, which can differ. There is evidence that clinicians reported lower severity of all skin symptoms compared to patients [62]. A limited number of five skin items were assessed during this study. One of the side effects not included was moist desquamation, in which the skin thins and looses its integrity. Further the knowledge about skin treatments such as creams and dressings after or prior to treatment and how well patients adhered to the prescribed application were not available.
Previous research has shown mixed results regarding the effectiveness of topical creams in preventing and treating radiation-induced skin reactions. While some studies report that general skincare and the use of anti-inflammatory cremes may reduce irritation, overall results remain inconsistent [63] [64]. Wound dressings that keep the skin moist, have shown supportive effects on healing, but no single treatment has been shown to be consistently effective [64]. In this study, further confounding factors such as BMI, tumor

size, breast size, and genetic factors were not evaluated. Previous studies have identified these variables as predictors of acute skin reactions after radiotherapy, with higher BMI and a breast size being associated with an increased risk of developing those reactions [55]. Further genetic factors have shown to influence the severity of radiation-induced skin reactions in breast cancer patients [65].

During the study period, both the treatment technique (3D-CRT to IMRT and VMAT) and the boost method (SQB to SIB) changed over time, however this temporal shift factor could not be modeled and was therefore not accounted for in the analysis. In *Experiment 2* and *Experiment 3* the ordinal PROs (scores 1–5) were dichotomized to indicate occurrence of worsening events. This approach, however, reduces the granularity of the information.

Minor variations in how participants interpreted the survey questions and answer scores cannot be ruled out. Although guidance was provided at the beginning of the study, compliance with these instructions was not monitored during the survey. This especially effected *Experiment 1*, where absolute scores were reported.

A further limitation was the different follow-up time after treatment start on the last fraction. For treatment plans without a boost or a SIB the last fraction follow-up was 4 weeks after the first fraction. For patients, who received a SQB, however, the last fraction and the survey follow-up were conducted one week later. In this case skin toxicities from the main treatment had already had one more week to to build up or subside.

# 6 Conclusion and Outlook

The aim of this thesis was to identify dosimetric and other confounding factors that influence the skin related side effects experienced by patients treated with radiotherapy for breast cancer at the Department of Radiation Oncology at the Medical University of Vienna / General Hospital of Vienna.

The most common response in all PRO items for acute skin toxicities was mild (score = 2) in all investigated combinations of treatment techniques and boost methods. The frequency of severe (score = 4) was at a maximum of 21%, while for most groups it remained below 15%. The frequency of score 5 (very severe) was below 6% for all items and groups, with only four exceptions of the 28 cases (4 items with a 5-score answering scale × 7 groups).

Overall, the multivariate logistic regression analysis demonstrated that $V_{40\mathrm{Gy}}$ is a consistent predictor of worsening acute side effects, while age acts as a mitigation factor. The remaining clinical variables (chemotherapy, hormone therapy, prior surgery and laterality) showed no systematic influence. In future treatment planning, segmenting the skin and trying to minimize high-dose skin volumes might be considered, as it could potentially reduce the occurrence of radiation-induced skin effects for breast cancer patients. Further, it may be beneficial to analyze the volumes associated with a significantly higher increase of skin toxicities in order to identify potential volume thresholds that could be incorporated into treatment planning and optimization. Such limits could be applied generally across all techniques or specifically for techniques, associated with a higher risk of more severe side effects.

As further analysis, the discrete pointwise dose-volume metrics could be replaced with continuous full DVH curves. This would enable a more holistic picture than the analysis of selective dose values. Further, instead of DVHs, Dose-Surface Histograms (DSHs) could be used for the analysis of skin toxicity, as the skin is an almost two-dimensional surface. The surface dose could provide a representation compared to volumetric approaches to study surface effects in the skin. A formalism for the computation of the DSH has been proposed by Palma and Cella [66] for improved modeling of radiation-induced skin reaction.

For both acute and long-term effects, the analysis of predictors, as performed in *Experiment 2* and *Experiment 3*, could be extended by dividing the data into the different treatment groups. This could include comparisons between groups with least and most severe toxicities, for example a no-boost group and a SQB group. In *Experiment 2* item 36_2 (radiation skin reaction) would be suitable for a more treatment specific regression model, as a high number of worsening events (318) was observed.

Future analyses of long-term side effects would be valuable since some patients in the cohort have not yet reached the follow-up time of 2 years. At the time this study was conducted, 285 patients had reached the final follow-up time, while 239 had not.

In a next step, radiomic features, which are quantitative measures extracted from medical images, could be considered as data metrics to identify factors that influence the severity or worsening of radiation-induced skin toxicities. A similar approach was demonstrated in a study by Feng et al. [67], where a machine learning model was developed to predict acute radiation skin reactions for breast cancer patients prior to radiotherapy based on radiomic features, clinical, and dosimetric data. Their results suggested that radiomic features contributed substantially to predictive outcome, while adding dosimetric values did not significantly improve the model's performance.

## Acronyms

**3D-CRT** Three-Dimensional Conformal Radiation Therapy.

**CT** Computed Tomography.

**CTCAE** Common Terminology Criteria for Adverse Events.

**CTV** Clinical Target Volume.

**DSHs** Dose-Surface Histograms.

**DVH** Dose-Volume Histograms.

**ER** Estrogen Receptor.

**GTV** Gross Tumor Volume.

**HDI** Human Development Index.

**HER2** Human Epidermal Growth Factor Receptor 2.

**IMRT** Intensity Modulated Radiation Therapy.

**Linac** Linear Accelerator.

**MC** Monte Carlo.

**OAR** Organs At Risk.

**PBC** Pencil Beam Convolution.

**PBI** Partial Breast Irradiation.

**PEDRO** Patient Experience Data in Radiation Oncology.

**PGR** Progesterone Receptor.

**PRO** Patient Reported Outcome.

**PTV** Planning Target Volume.

**SIB** Simultaneous Integrated Boost.

**SQB** Sequential Boost.

**TERMA** Total Energy Released per unit MAss.

**TNM** Tumor-Node-Metastasis.

**TPS** Treatment Planning System.

**VMAT** Volumentric Modulated Arc Therapy.

**WBI** Irradiation of the Whole Breast.

# List of Tables

# List of Figures

## References


[1] World Health Organization. *Breast cancer*. https://www.who.int/news-room/fact-sheets/detail/breast-cancer. accessed on 26.08.2025.

[2] C. Gómez-Raposo, F. Zambrana Tévar, M. Sereno Moyano, M. López Gómez, and E. Casado. "Male breast cancer". In: *Cancer Treatment Reviews* 36 (2010), pp. 451–457. DOI: 10.1016/j.ctrv.2010.02.002.

[3] C. Wild and B.W.Stewart. *World Cancer Report 2014*. Tech. rep. ISBN: 978-92-832-0429-9. World Health Organization, (2014).

[4] D. Boyce-Fappiano, I. Bedrosian, Y. Shen, H. Lin, O. Gjyshi, and A. Yoder et al. "Evaluation of overall survival and barriers to surgery for patients with breast cancer treated without surgery: a National Cancer Database analysis". In: *NPJ Breast Cancer* (2021). DOI: 10.1038/s41523-021-00294-w.

[5] R. Atun, D. Jaffray, M. Barton, F. Bray, M. Baumann, and B. Vikram et al. "Expanding global access to radiotherapy". In: *The Lancet Oncology Commission* 16 (2015), pp. 1153–1186. DOI: 10.1016/S1470-2045(15)00222-3.

[6] R. Baskar, J. Dai, N. Wenlong, R. Yeo, and K. Yeoh. "Biological response of cancer cells to radiation treatment". In: *Frontiers in Molecular Biosciences* 1 (2014). DOI: 10.3389/fmolb.2014.00024.

[7] S. Baatout. *Radiobiology Textbook*. Springer, (2023). Chap. 6. ISBN: 9783031188091.

[8] J. Wei, L. Meng, X.Hou, C. Qu, Y. Xin, and X. Jiang. "Radiation-induced skin reactions: mechanism and treatment." In: *Cancer management and research* (2018), pp. 167–177. DOI: 10.2147/CMAR.S188655.

[9] K. Sjövall, G. Strömbeck, A. Löfgren, P. Bendahl, and B. Gunnars. "Adjuvant radiotherapy of women with breast cancer – Information, support and side-effects". In: *European Journal of Oncology Nursing* 14 (2010), pp. 147–153. DOI: https://doi.org/10.1016/j.ejon.2009.09.002.

[10] E. Lam, C. Yee, G. Wong, M. Popovic, L. Drost, and K. Pon et al. "A systematic review and meta-analysis of clinician-reported versus patient-reported outcomes of radiation dermatitis". In: *The Breast* 50 (2020), pp. 125–134. DOI: 10.1016/j.breast.2019.09.009.

[11] G. Heilemann, D. Georg, M. Dobiasch, J. Widder, and A. Renner. "Automation of ePROMs in radiation oncology and its impact on patient response and bias". In: *Radiotherapy and Oncology* 199 (2024), p. 110427. DOI: 10.1016/j.radonc.2024.110427.

[12] F. Khan. *The physics of radiation therapy*. Lippincott Williams & Wilkins, (2003). Chap. 5.

[13] International Atomic Energy Agency. *Radiation Oncology Physics: A Handbook for Teachers and Students*. IAEA, (2005). Chap. 1.

[14] International Atomic Energy Agency. *Commissioning and Quality Assurance of Computerized Planning Systems for Radiation Treatment of Cancer*. Tech. rep. IAEA, (2004).

[15] G. Choppin, J. Liljenzin, and J. Rydberg. *Absorption of Nuclear Radiation*. Third Edition. Woburn: Butterworth-Heinemann, (2002), pp. 123–165. DOI: 10.1016/B978-075067463-8/50006-6.

[16] R. Evans. *The Atomic Nucleus*. McGraw-Hill Publishing, (1955).

[17] A. Ahnesjö and M. Aspradakis. "Dose calculations for external photon beams in radiotherap". In: *Physics in Medicine & Biology* 44 (1999). DOI: 10.1088/0031-9155/44/11/201.

[18] Faiz M. Khan. *The physics of radiation therapy*. Lippincott Williams & Wilkins, (2003). Chap. 9.

[19] T. FitzGerald. *Radiation Therapy*. IntechOpen, (2023). Chap. 1. DOI: 10.5772/intechopen.104154.

[20] Z. Chen, M. Dominello, M. Joiner, and J. Burmeister. "Proton versus photon radiation therapy: A clinical review". In: *Frontiers in Oncology* 13 (2023). DOI: 10.3389/fonc.2023.1133909.

[21] National Cancer Institute. *Radiation Therapy to Treat Cancer*. https://www.cancer.gov/about-cancer/treatment/types/radiation-therapy. accessed on 18.10.2025.

[22] R. Mohan and D. Grosshans. "Proton therapy – Present and future". In: *Advanced Drug Delivery Reviews* 109 (2017). Radiotherapy for cancer: present and future, pp. 26–44. DOI: 10.1016/j.addr.2016.11.006.

[23] P. DeLuca. "The International Commission on Radiation Units and Measurements". In: *Journal of the ICRU* 7 (2 2007). DOI: 10.1093/jicru_ndn001.

[24] N. Burnet, S. Thomas, K. Burton, and S. Jefferies. "Defining the tumour and target volumes for radiotherapy." In: *Cancer imaging : the official publication of the International Cancer Imaging Society* 4 (2004), pp. 153–61. DOI: 10.1102/1470-7330.2004.0054.

[25] D. Kim, K. Park, H. Kim, and J. Kim. "History of the Photon Beam Dose Calculation Algorithm in Radiation Treatment Planning System". In: *Progress in Medical Physics* 31 (2020), pp. 54–62. DOI: 10.14316/pmp.2020.31.3.54.

[26] T. Yang, R. Taob, P. Elkhuizenc, C. van Vliet-Vroegindeweijc, G. Lid, and S. Powell. "Tumor bed delineation for external beam accelerated partial breast irradiation: A systematic review". In: *Radiotherapy and Oncology* 108 (2013). DOI: 10.1016/j.radonc.2013.05.028.

[27] M. Dzhugashvili, L. Veldeman, and A. Kirby. "The role of the radiation therapy breast boost in the 2020s." In: *The Breast* 69 (2023), pp. 299–305. DOI: 10.1016/j.breast.2023.03.009.

[28] B. Cho. "Intensity-modulated radiation therapy: a review with a physics perspective." In: *Radiation Oncology Journal* 36 (2018). DOI: 10.3857/roj.2018.00122.

[29] Johns Hopkins Medicine Pathology. *John Hopkins University Medicine*. https://pathology.jhu.edu/breast/staging-grade/. accessed on 23.09.2025.

[30] B. Mahul, F. Greene, S. Edge, C. Compton, J. Gershenwald, and R. Brookland et al. "The Eighth Edition AJCC Cancer Staging Manual: Continuing to build a bridge from a population-based to a more "personalized" approach to cancer staging". In: *CA: A Cancer Journal for Clinicians* 67 (2017), pp. 93–99. DOI: 10.3322/caac.21388.

[31] M. Amin, S. Edge, F. Greene, D. Byrda, R. Brooklanda, and M. Washington et al. *AJCC Cancer Staging Manual*. 8th ed. Springer, (2017). ISBN: 978-3-319-40617-6.

[32] Cancer Research UK. *TNM staging for breast cancer*. https://www.cancerresearchuk.org/about-cancer/breast-cancer/stages-grades/tnm-staging. accessed on 23.09.2025.

[33] N. Harbeck, F. Penault-Llorca, J. Cortes, M. Gnant, N. Houssami, and P. Poortmans et al. "Breast cancer". In: *Nature Reviews Disease Primers* 5 (2019). DOI: https://doi.org/10.1038/s41572-019-0111-2.

[34] M. Dowsett, T. Nielsen, R. A'Hern, J. Bartlett, R. Coombes, and J. Cuzick et al. "Assessment of Ki67 in Breast Cancer: Recommendations from the International Ki67 in Breast Cancer Working Group". In: *Journal of the National Cancer Institute* 103 (2011), pp. 1656–1664. DOI: 10.1093/jnci/djr393.

[35] T. Choh Man. "Data, Data, Everywhere: Statistical Issues in Data Mining". In: *Philosophy of Statistics*. Vol. 7. Handbook of the Philosophy of Science. North-Holland, (2011). DOI: /10.1016/B978-0-444-51862-0.50034-4.

[36] Y. Benjamini and Y.Hochberg. "Controlling the False Discovery Rate: a Practical and Powerful Approach to Multiple Testing". In: *Journal of the Royal Statistical Society B* 57 (1995), pp. 289–300. DOI: 10.1111/j.2517-6161.1995.tb02031.x.

[37] U.S. Department of Health and Human Services NIH. *Patient-Reported Outcomes version of the Common Terminology Criteria for Adverse Events (PRO-CTCAE)*. https://healthcaredelivery.cancer.gov/pro-ctcae/. accessed on 28.08.2025.

[38] *About DICOM: Overview*. https://www.dicomstandard.org/about-home. accessed on 2.10.2025.

[39] D. Mason. "SU-E-T-33: pydicom: an open source DICOM library". In: *Medical Physics* 38 (2011), p. 3493. DOI: 10.1118/1.3611983.

[40] A. Chanda and G. Singh. "Skin". In: *Mechanical Properties of Human Tissues*. Singapore: Springer Nature Singapore, (2023), pp. 13–23. DOI: 10.1007/978-981-99-2225-3_2.

[41] P. Virtanen, R. Gommers, T. Oliphant, T. Reddy M. Haberland, and D. Cournapeau et al. "SciPy 1.0: fundamental algorithms for scientific computing in Python". In: *Nature Methods* 17 (2020), pp. 261–272. DOI: 10.1038/s41592-019-0686-2.

[42] S. Seabold and J. Perktold. "statsmodels: Econometric and statistical modeling with python". In: *Proceedings of the 9th Python in Science Conference*. 2010, pp. 92 –96. DOI: 10.25080/Majora-92bf1922-011.

[43] J. Maduro, E. Pras, P. Willemse, and E. de Vries. "Acute and long-term toxicity following radiotherapy alone or in combination with chemotherapy for locally advanced cervical cancer". In: *Cancer Treatment Reviews* 29 (2003), pp. 471–488. DOI: 10.1016/S0305-7372(03)00117-8.

[44] C. Davidson-Pilon. "lifelines: survival analysis in Python". In: *Journal of Open Source Software* 4 (2019), p. 1317. DOI: 10.21105/joss.01317.

[45] K. Borm, M. Loos, M. Oechsner, M. Mayinger, D. Paepke, and M. Kiechle et al. "Acute radiodermatitis in modern adjuvant 3D conformal radiotherapy for breast cancer - the impact of dose distribution and patient related factors". In: *Radiation Oncology* 13 (2018). DOI: 10.1186/s13014-018-1160-5.

[46] S. Thomson, J. Alsner, H. Nielsen, E. Jakobsen, M. Nielsen, and M. Møller et al. "Volume matters: Breast induration is associated with irradiated breast volume in the Danish Breast Cancer Group phase III randomized Partial Breast Irradiation trial". In: *Radiotherapy and Oncology* 177 (2022), pp. 231–235. DOI: 10.1016/j.radonc.2022.09.024.

[47] C. Zhong, M. Huang, J. Yuan, R. Xie, H. Yu, and Z. Lai et al. "Sequential or simultaneous-integrated boost in early-stage breast cancer patients: trade-offs between skin toxicity and risk of compromised coverage". In: *Radiation Oncology* 20 (2025). DOI: 10.1186/s13014-025-02584-0.

[48] M. Guerrero, X. Li, M. Earl, M. Sarfaraz, and E. Kiggundu. "Simultaneous integrated boost for breast cancer using imrt: a radiobiological and treatment planning study". In: *International Journal of Radiation Oncology, Biology, Physics* 59 (2004), pp. 1513–1522. DOI: 10.1016/j.ijrobp.2004.04.007.

[49] H. van der Laan, W. Dolsma, J. Maduro, E. Korevaar, M. Hollander, and J. Langendijk. "Three-Dimensional Conformal Simultaneously Integrated Boost Technique for Breast-Conserving Radiotherapy". In: *International Journal of Radiation Oncology, Biology, Physics* 68 (2007), pp. 1018–1023. DOI: 10.1016/j.ijrobp.2007.01.037.

[50] H. Park, D. Kang, T. Lee, and D. Oh. "Dynamics in distress and quality of life in patients undergoing radiation therapy: a prospective cohort study". In: *Supportive Care in Cancer* 33 (2025). DOI: 10.1007/s00520-025-09371-3.

[51] D. Kang, I. Kim, Y. Im, Y. Park, J. Ahn, and J. Lee et al. "Quantitative changes in skin composition parameters due to chemotherapy in breast cancer patients: a cohort study". In: *Epidemiology* 152 (2015), pp. 675–682. DOI: 10.1007/s10549-015-3502-4.

[52] D. Porock and L. Kristjanson. "Skin reactions during radiotherapy for breast cancer: the use and impact of topical agents and dressings". In: *European Journal of Cancer Care* 8 (1999), pp. 143–153. DOI: 10.1046/j.1365-2354.1999.00153.x.

[53] P. Ciammella, A. Podgornii, M. Galeandro, R. Micera, D. Ramundo, and T. Palmiero et al. "Toxicity and cosmetic outcome of hypofractionated whole-breast radiotherapy: predictive clinical and dosimetric factors". In: *Radiation Oncology* 9 (2014). DOI: 10.1186/1748-717X-9-97.

[54] U. Kraus-Tiefenbacher, A. Sfintizky, G. Welzel, A. Simeonova, E. Sperk, and K. Siebenlist et al. "Factors of influence on acute skin toxicity of breast cancer patients treated with standard three-dimensional conformal radiotherapy (3D-CRT) after breast conserving surgery (BCS)". In: *Radiation Oncology* 7 (2012). DOI: 10.1186/1748-717X-7-217.

[55] E. Córdoba, E. Lacunza, and A. Güerci. "Clinical factors affecting the determination of radiotherapy-induced skin toxicity in breast cancer". In: *Radiation Oncology Journal* 39 (2021), pp. 315–323. DOI: 10.3857/roj.2020.00395.

[56] V. Bruzzaniti, P. Pinnarò A. Abate, M. D'Andrea, E. Infusino, and V. Landoni et al. "Dosimetric and clinical advantages of deep inspiration breath-hold (DIBH) during radiotherapy of breast cancer". In: *Journal of Experimental & Clinical Cancer Research* 32 (2013). DOI: 10.1186/1756-9966-32-88.

[57] A. Cicchetti, P. Mangili, A. Fodor, M. Gabellini, A. Chiara, and C. Deantoni et al. "Skin dose-volume predictors of moderate-severe late side effects after whole breast radiotherapy". In: *Radiotherapy and Oncology* 194 (2024), p. 110183. DOI: 10.1016/j.radonc.2024.110183.

[58] F. De Rose, A. Fogliata, D. Franceschini, C. Iftode, A. D'Agostino, and T. Comito et al. "Hypofractionated whole breast irradiation and simultaneous integrated boost in large-breasted patients: long-term toxicity and cosmesis". In: *Clinical Breast Cancer* 20 (2020), pp. 527–533. DOI: 10.1016/j.clbc.2020.06.005.

[59] L. Court, R. Tishler, A. Allen, H. Xiang, M. Makrigiorgos, and L. Chin. "Experimental evaluation of the accuracy of skin dose calculation for a commercial treatment planning system". In: *Journal of Applied Clinical Medical Physics* 9 (2008), pp. 29–35. DOI: 10.1120/jacmp.v9i1.2792.

[60] M. Toossi, N. Mohamadiana, M. Mohammadif, M. Ghorbani, M. Hassani, and B. Khajetashd et al. "Assessment of skin dose in breast cancer radiotherapy: on-phantom measurement and Monte Carlo simulation". In: *Reports of Practical Oncology and Radiotherapy* 25 (2020), pp. 456–461. DOI: 10.1016/j.rpor.2020.03.008.

[61] F. Holt, A. Ivanova, Z. Wang, S. Darby, F. Duane, and G. Ntentas et al. "Estimated Doses to the Heart, Lungs and Oesophagus and Risks From Typical UK Radiotherapy for Early Breast Cancer During 2015–2023". In: *Clinical Oncology* 36 (2024), pp. 322–332. DOI: 10.1016/j.clon.2024.05.002.

[62] T. Behrooziana, L. Miltona, L. Zhangb, J. Loub, I. Karama, and E. Lama et al. "How do patient-reported outcomes compare with clinician assessments? A prospective study of radiation dermatitis in breast cancer". In: *Radiotherapy & Oncology* 159 (2021), pp. 98–105. DOI: 10.1016/j.radonc.2021.03.020.

[63] F. Bray, B. Simmons, A. Wolfson, and K. Nouri. "Acute and Chronic Cutaneous Reactions to Ionizing Radiation Therapy". In: *Dermatology and Therapy* 6 (2016), pp. 185–206. DOI: 10.1007/s13555-016-0120-y.

[64] F. Hegedus, L. Mathew, and R. Schwartz. "Radiation dermatitis: an overview". In: *International Journal of Dermatology* 56 (2016), pp. 909–914. DOI: 10.1111/ijd.13371.

[65] A. Borghini, C. Vecoli, A. Mercuri, M. Petruzzelli, M. D'Errico, and M. Portaluri et al. "Genetic risk score and acute skin toxicity after breast radiation therapy". In: *Cancer Biotherapy & Radiopharmaceuticals* 29 (2014), pp. 267–272. DOI: 10.1089/cbr.2014.1620.

[66] G. Palma and L. Cella. "A new formalism of Dose Surface Histograms for robust modeling of skin toxicity in radiation therapy". In: *Physica Medica: European Journal of Medical Physics* 59 (2020), pp. 75 –78. DOI: 10.1016/j.ejmp.2019.02.005.

[67] H. Feng, H. Wang, L. Xu, Y. Ren, Q. Ni, and Z. Yang et al. "Prediction of radiation-induced acute skin toxicity in breast cancer patients using data encapsulation screening and dose-gradient-based multi-region radiomics technique: A multicenter study". In: *Frontiers in Oncology* 12 (2022). DOI: 10.3389/fonc.2022.1017435.